UNIVERSITA' DEGLI STUDI
DI PADOVA
Dipartimento di Fisica e Astronomia
Dipartimento di Ingegneria Industriale

ISTITUTO NAZIONALE
DI FISICA NUCLEARE
Laboratori Nazionali di Legnaro

Under the Auspice of the TESLA TECHNOLOGY COLLABORATION

MASTER THESIS

in

"Surface Treatments for Industrial Applications"

Sputtering of Molybdenum thick films for cyclotron targets to produce Technetium-99m

Supervisor: Prof. V. Palmieri

Co-Supervisor: Dott. Hanna Skliarova

Student: Sara Cisternino

N. Matr.: 1111605

Academic Year 2014-2015

Contents

Abstract

^{99m}Tc is the principal radioisotope used in medical diagnostics worldwide. Its 6-hour physical half-life and the 140 keV photopeak makes it ideally suited to medical imaging using conventional gamma cameras. ^{99m}Tc is derived from its parent element ^{99}Mo that is derived almost exclusively from the fission of uranium-235 targets (using primarily highly-enriched uranium) irradiated in a small number of old-aged research nuclear reactors.

A global shortage of ^{99}Mo exposed vulnerabilities in the supply chain of medical radioisotopes, therefore, individual countries and companies are exploring options for a future supply of medical radioisotopes. Cyclotron-based production of ^{99m}Tc starting from ^{100}Mo by ^{100}Mo(p,2n)^{99m}Tc reaction has been developed and evaluated at National Institute of Nuclear Physics – Legnaro National Laboratory (LNL-INFN); however some issues must be resolved. Among them innovative target development, because different requirements should be considered:

- target strength;
- ability to achieve desired thickness of target material;
- adherence of target material to baking;
- chemical resistance of backing;
- thermal performance at desired current.

Target design strategies, which have been identified in literature, include evaporation, e-beam melting, rolling of thick/self-supported targets, sintering, and electrodeposition. However, they are not performing good enough from the heat conduction point of view. In fact, the resulting targets have high oxidation level and low density, and the deposition technique does not allow to control the thickness and to deposit onto specific substrates [6].

The purpose of this thesis is the development of an innovative target based on the deposition of the target material, specifically Mo, by magnetron sputtering technique in order to provide high density, thick, uniform and adherent film onto chemically inert backing, as sapphire.

After the sputtering parameter optimization, thick (~100 μm) Mo films have been obtained and neither stress nor delamination have been observed.

Successful irradiations were carried out with 16 MeV cyclotron in Sant'Orsola Hospital, in Bologna, with different current beams. In fact, the system has performed at a current of more than 20 μA.

The γ-spectroscopy of the solution after the dissolution of irradiated target, in H_2O_2, has proved the inertness of sapphire both from the point of view of inertness under the beam, and from the chemical point of view.

Chapter 1

Radiopharmaceuticals and their radioisotopes production

Nuclear medicine is a medical modality that uses nuclear properties of radionuclides to diagnose diseases and treat disorders like cancer; radioactivity, indeed, can contribute to both diagnosis and therapy, respectively for its high detection sensitivity and through the biological effects of radiation.

Radionuclides are unstable atoms due to the unbalance between protons and neutrons in their nuclei. They spontaneously decay to reach a stable form by means of nuclear transition emitting radiation (Figure 1).

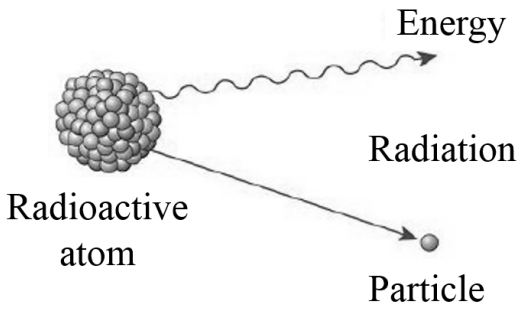

Figure 1 Radionuclide.

Radioisotopes have important uses in medical diagnosis, therapeutic treatment, and research.

It is essential that a given radionuclide is concentrated in the adequate area in the organism. Usually, this is achieved by attaching it to a chemical ligand that is selectively absorbed by specific organs or tissues. The chemical with the attached radionuclide is usually denoted as a radiopharmaceutical.

After a certain time after its introduction into the body, it is accumulated in the desired spot. The emitted radiation penetrates the tissues and it is finally detected by an external counting device. Scintigraphic images do not depend on morphological alterations; they may provide information on biological pathways at the deepest molecular level, but without perturbing those biochemical networks always operating in a living integrated system.

For nuclear diagnostic two fundamental methods have been developed:

- Single Photon Computed Emission Tomography (SPECT) that makes use of γ-emitting radionuclides (^{99m}Tc, ^{123}I, ^{67}Ga, ^{111}In, etc.);
- Positron Emission Tomography (PET) that uses radionuclides that decay through the emission of positrons (antiparticles of the electron) from which, following annihilation, two photons γ will generate (F^{18}, C^{11}, N^{13}, O^{15}, Ga^{68}, ^{82}Ru, etc.) [1].

The sources of radionuclides (Table 1) are:

- Naturally occurring radionuclides;
- Radionuclides produced by cyclotron;
- Generator radionuclides;
- Radionuclides produced by reactor:
    - By irradiation
    - Products of uranium fission.

Table 1 Medical isotopes commonly used for diagnostic imaging.

Isotope	Medical Use	Half-life	Typical Production Method
Tc – 99m	SPECT	6 hr	(Mo-99 from reactor), generator
I-123	SPECT	13.2 hr	Cyclotron, generator
Ga-67	SPECT	78.3 hr	Cyclotron
Th-201	SPECT	73.1 hr	Cyclotron
In-111	SPECT	2.8 d	Cyclotron
Xe-127	SPECT	36 d	Cyclotron
Co-57	SPECT	272 d	Cyclotron
C-11	PET	20 min	Cyclotron
N-13	PET	10 min	Cyclotron
O-15	PET	2 min	Cyclotron
F-18	PET	110 min	Cyclotron
Ga-68	PET	68 min	Ge-68 via cyclotron
Ru-82	PET	1.3 min	Sr-82 via cyclotron

1.1 Technetium

1.1.1 The advantage of Technetium in nuclear Medicine

Technetium-99m (^{99m}Tc) is used in approximately 85% of nuclear medicine diagnostic imaging procedures worldwide since it has got excellent physical and chemical properties that make it applicable in a large variety of indications:

- 6.01 hours half-life, enough for radiopharmaceutical preparation, patient administration and clinical exam execution; on the other hand it is short enough to provide acceptable dose to the patient;
- E_γ = 140 keV;
- adequate for the incorporation in many molecules probe;
- versatility for different diagnostic investigations depending on the molecule with which it is associated;
- applicability of use because it is available through a ^{99}Mo/^{99m}Tc generator system.

^{99m}Tc is a versatile element that supports a spectrum of different radiopharmaceuticals targeting multiple disease sites, in particular bone, cardiac, renal, lung and endocrine disorders.

1.2 Production of Technetium

1.2.1 ^{99}Mo/^{99m}Tc generator

^{99m}Tc is commonly available in a generator form. A ^{99}Mo/^{99m}Tc generator (Figure 2), or 'technetium generator', is a device used to recover and concentrate technetium from ^{99}Mo.

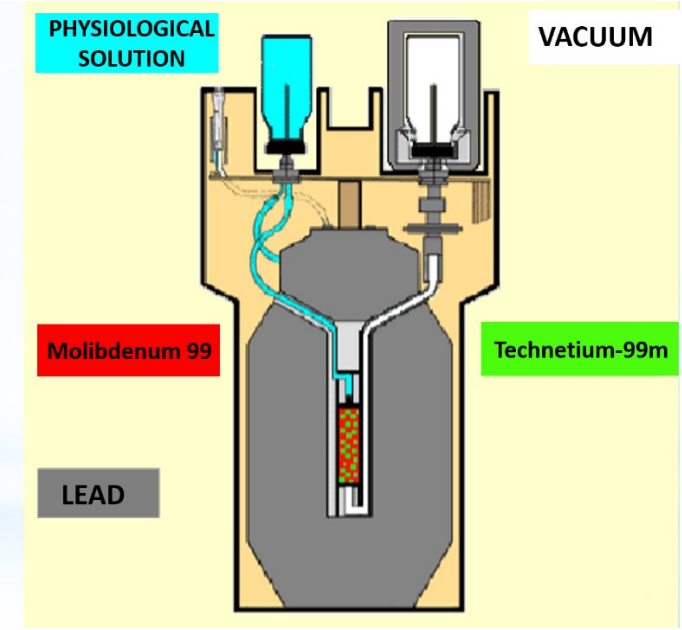

Figure 2 Schematic representation of $^{99}Mo/^{99m}Tc$ generator.

A conventional generator consists of an alumina (Al_2O_3) column about the size of a short pencil, associated tubing, valves and filters for extracting technetium, and lead shielding for radiation protection.

The column is loaded with ^{99}Mo at the generator manufacturing facility before being shipped to a hospital, radiopharmacy or clinic.

The ^{99}Mo in the column decays technetium with about a 66 hours half-life. About 88.6% of the ^{99}Mo decays to ^{99m}Tc; the remainder decays to ^{99g}Tc (Figure 3). Technetium is eluted by passing a saline solution through the column.

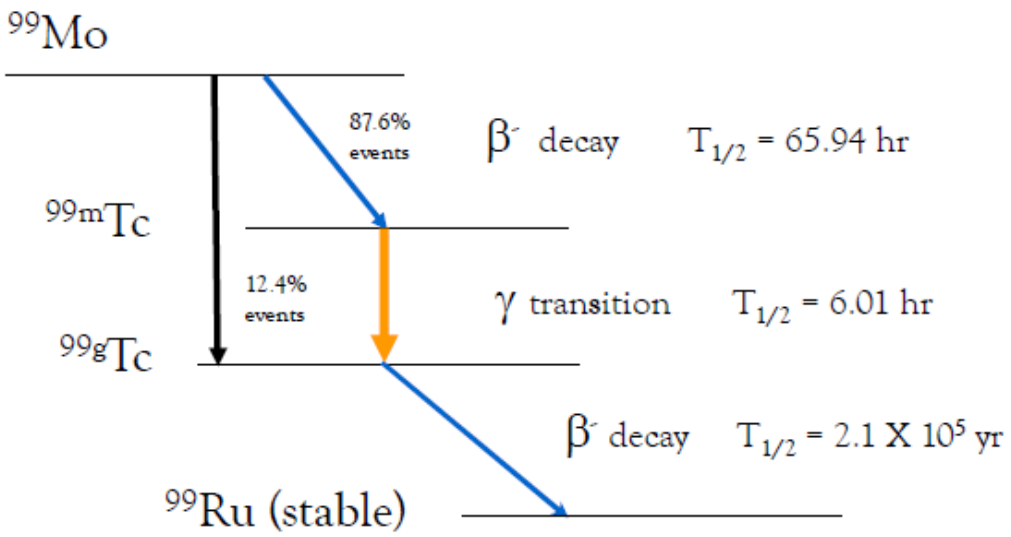

Figure 3 ^{99}Mo decay chain

^{99}Mo and ^{99m}Tc are in transient equilibrium because the half-life of ^{99}Mo is about 10 times longer than of ^{99m}Tc, so in the generator, after 24 h the daughter activity reaches a substantial equilibrium with the parent one.

Daily extraction of pertechnetate [^{99m}Tc]TcO_4^- from generators allows to use it directly or to label other molecules to obtain different radiopharmaceuticals. Indeed, ^{99m}Tc-pertechnetate is used for thyroid imaging, but most applications involve incorporating the ^{99m}Tc in selected carriers with commercially available kits to yield specific ^{99m}Tc radiopharmacauticals suitable for planar (2D) scintigraphic imaging and 3D SPECT of major medical conditions, such as heart and lung function and cancer.

1.2.1.1 Problem of Molybdenum generator precursor from nuclear plants

The shortage in availability of ^{99m}Tc for diagnostic imaging is due to the complexity of the supply chain that involves many steps (Figure 4):

- Uranium target manufacturing;
- Target irradiation in a suitable nuclear reactor (Figure 5);
- Processing to dissolve the irradiated targets and chemically extract ^{99}Mo;
- ^{99}Mo/^{99m}Tc generator manufacturing;
- Elution of ^{99m}Tc from the generators and preparation of radiopharmaceuticals in a radiopharmacy;
- Transport of radiopharmaceuticals to the end user clinics.

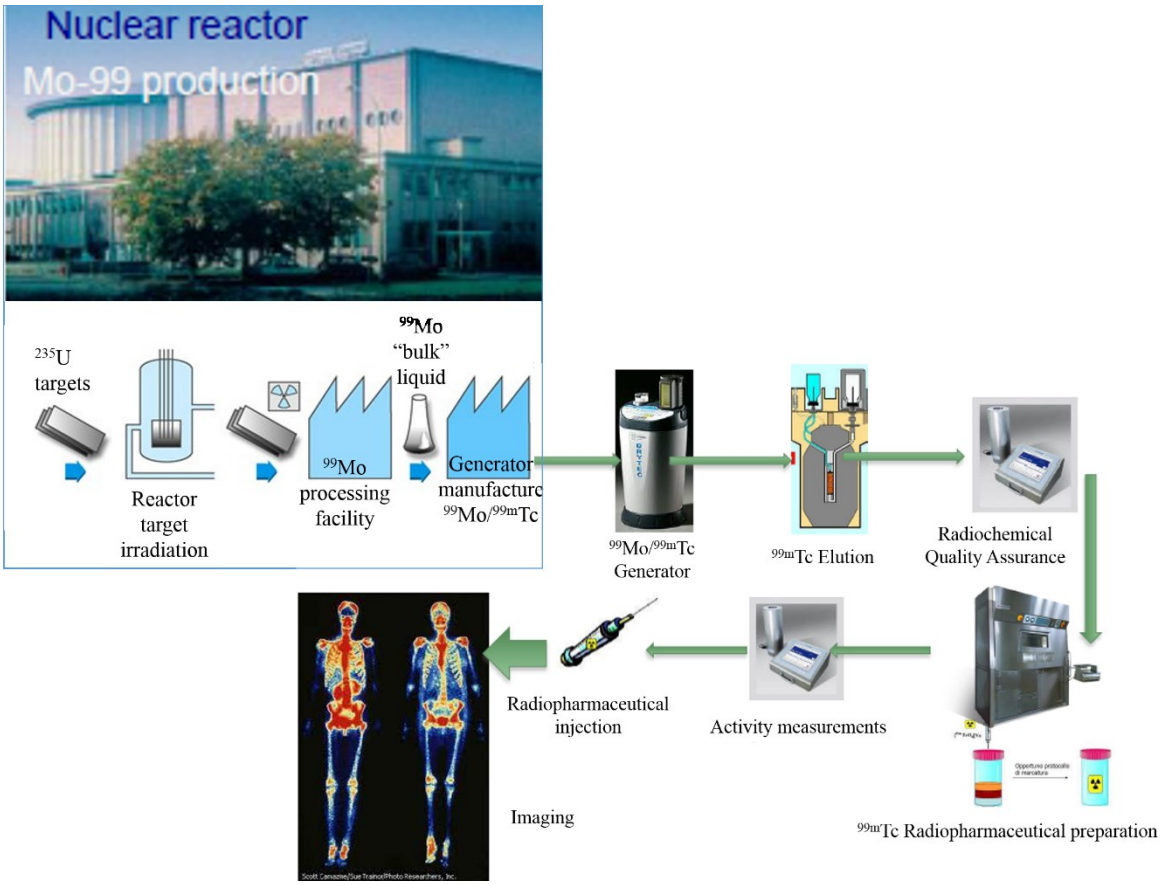

Figure 4 ^{99m}Tc production chain.

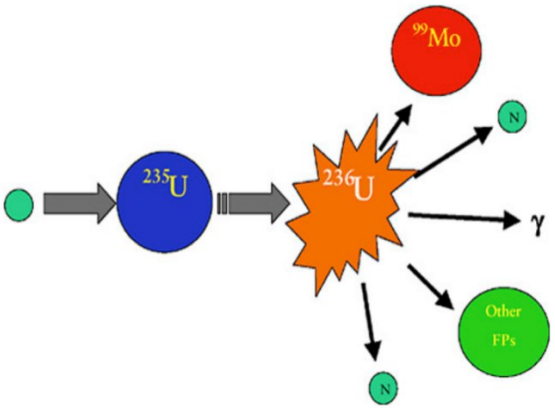

Figure 5 Current massive production method of ^{99}Mo.

Therefore, the majority of the ^{99m}Tc used for medical imaging is produced from the decay of ^{99}Mo, in turn produced in nuclear reactors by the fission and recovery of ^{99}Mo from ^{235}U (highly enriched uranium, HEU).

The fragility of ^{99}Mo supply has recently come to light during recent shutdowns at two leading production sites: the research reactor NRU at Chalk River, Ontario (Canada), and the

HFR reactor at Petten (The Netherlands) [2], [3]. However, these reactors are more than fifty years old and they have become unreliable with several recent unexpected shutdowns.

Moreover, they run using highly enriched (weapons grade) uranium fuel (HEU) for the production of ^{99}Mo. HEU represents a proliferation risk and thus there are significant security issues associated with the current route of production.

Existing reactors will be required to use low enriched uranium (LEU) which contains less than 20% ^{235}U. However, with less than 20% ^{235}U in the targets, there will be no doubt about the reduction in the output of ^{99}Mo making difficult to keep up with the daily demands for ^{99m}Tc [4].

For these reasons, the future of ^{99}Mo/^{99m}Tc production will require alternative routes of production.

1.2.2 Production of ^{99m}Tc by cyclotron

All the radionuclides of medical interest are obtained through generators and cyclotrons.

Cyclotron is a particle accelerator, used to produce high-energy beams of particles exploited to occur reactions. Figure 6 shows the operating principle of a cyclotron.

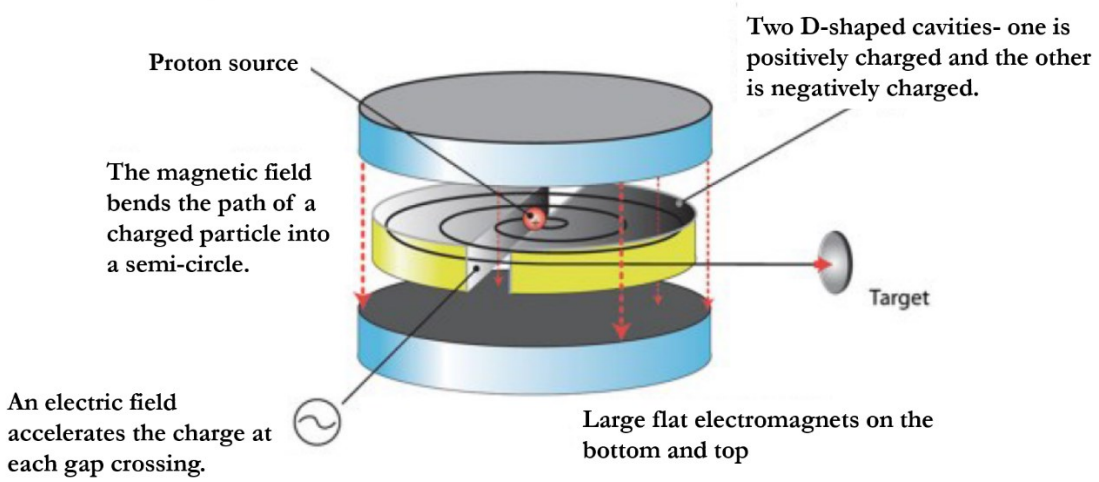

Figure 6 Operating principle of a cyclotron.

Because of the recent shortage in the reactor production of ^{99}Mo, alternative methods involving cyclotrons have been studied [5].

Several reactions were investigated [3] for the production of ^{99m}Tc, directly or indirectly, via production of ^{99}Mo:

1. Parent ^{99}Mo production
    - **^{100}Mo(p,pn)^{99}Mo**: Resulted yields too small to be considered as a viable alternative;
    - **^{100}Mo(γ,n)^{99}Mo**: For this option the electron beam should be converted to a photon beam via bremsstrahlung. This method cannot provide high specific activity and therefore it does not permit the use of standard Mo/Tc generators [6].
    - **^{98}Mo(n,γ)^{99}Mo**: The resulting ^{99}Mo specific activities, both at saturation and after the first 24 hours irradiation, are too much low to consider a massive production using such a system. High ^{98}Mo-enriched mass is required for the irradiated sample;
    - **^{100}Mo(n,2n)^{99}Mo**: High-energy neutrons for this reaction are provided by energetic deuterons bombarding a natural carbon target. The use of this type of neutron source and the expected ^{99}Mo production level using such a reaction route is currently not favorable.
2. Direct ^{99m}Tc production
    - **^{98}Mo(d,n)^{99m}Tc** : Productions expected by deuteron reactions have shown to be not competitive respect other routes;
    - **^{98}Mo(p,γ)^{99m}Tc** : This reaction route provides a low contribution to the ^{99m}Tc direct production compared with the other competitor direct reaction channels;
    - **^{100}Mo(p,2n)^{99m}Tc**: in this route ^{99m}Tc is directly produced for immediate use, via the reaction of an accelerated proton with a ^{100}Mo nucleus yielding ^{99m}Tc and two neutrons. This is only useful for a local production because ^{99m}Tc is a short-lived radioisotope.

1.2.2.1 ^{100}Mo - ^{99m}Tc reaction as chosen one in LNL

The National Institute of Nuclear Physics – Legnaro National Laboratory – is among the research groups involved in the investigation of the alternative and more flexible production routes, based on accelerators for ^{99m}Tc production.

Two main alternative routes have been investigated, based upon [3]:

- ^{99}Mo production by accelerator-driven neutron sources;

- ^{99}Mo/^{99m}Tc direct production.

The nuclides production could be outlined as in the following sketch shown in Figure 7.

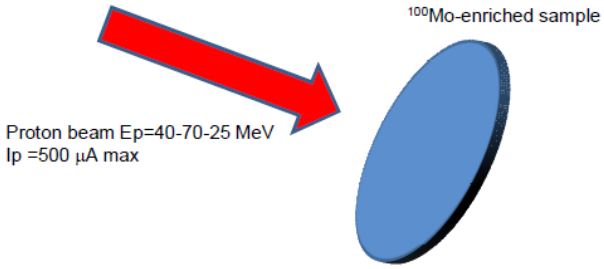

Figure 7 Proof-of-principle scheme for ^{99}Mo/^{99m}Tc direct production using ^{100}Mo sample target [3].

After preliminary evaluations the reaction ^{100}Mo(p,2n)^{99m}Tc was chosen for the direct ^{99m}Tc production without passing through ^{99}Mo precursor because the other reactions are not competitive. Feasibility of cyclotron production of ^{99m}Tc via the ^{100}Mo(p,2n)^{99m}Tc reaction was demonstrated in the early seventies [7].

The goal is to get some indications about a possible future supply of such radionuclides in Italy, taking into account the new powerful 70 MeV cyclotron available at LNL for nuclear physics research programs.

The radionuclide decay time being short enough ($T_{1/2}$ = 6 h), a production system may however still be conceived although limited to regional users (medical centers) surrounding the production plant.

Such a reaction route has recently been proposed as one of the feasible way to meet the future demand of ^{99m}Tc.

^{100}Mo(p,2n)^{99m}Tc reaction offers potential opportunities to get interesting amounts of ^{99m}Tc using high current (500 μA) cyclotrons with output energies about 20-25 MeV.

Experimental measurements have been carried out in recent years, in order to better determine the impurities produced by other open reaction channels during irradiation. Among all the impurities produced inside the sample, the ones detected having the longest half-life that would remain in the final product because of the same chemical species are the ^{95}Tc ($T_{1/2}$ = 20 h), ^{95m}Tc ($T_{1/2}$ = 60 d), ^{97m}Tc ($T_{1/2}$ = 91.0 d), ^{96}Tc ($T_{1/2}$ = 4.28 d). However, at the end of the preparation process, the contribution given by ^{95}Tc and ^{96}Tc could be considered negligible.

The direct production of ^{99m}Tc is therefore interesting for energies below 25 MeV to minimize the impurities.

However, still an unknown and key issue, is the amount of the ground state, pure β-emitter, ^{99g}Tc which is hard to be determined, being also produced by the same ^{100}Mo(p,2n) reaction. As can be drawn by the plot in Figure 8, the production rate in the 25-10 MeV range for such a long-lived isomer ($T_{1/2}$ = 2,1·10^5 y), which is useless for diagnostic procedure, is expected to be in excess of a factor 3 than ^{99m}Tc according to the only theoretical excitation function available from TENDL2009 library.

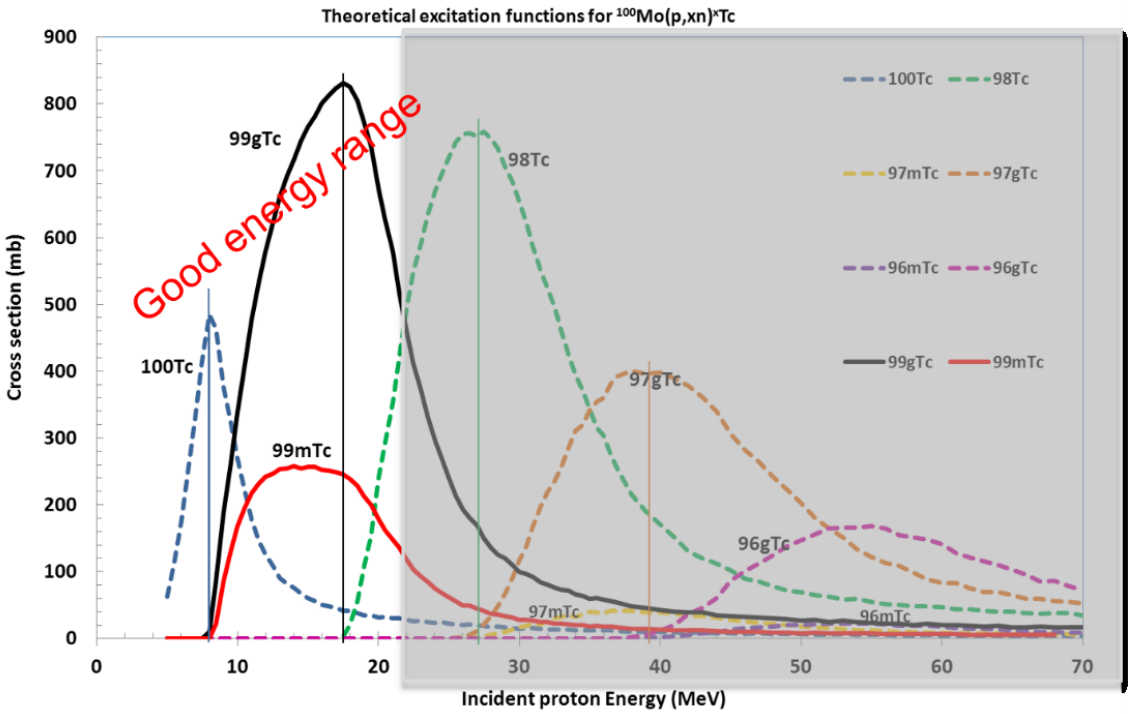

Figure 8 Theoretical excitation function for ^{100}Mo(p,xn)^{x}Tc.

The nuclides ratio R= N^{99gTc}/N^{99mTc} > 4 is in fact generally reported to interfere with the functions of some labeled radiopharmaceuticals, reducing the effectiveness of Tc-based scans.

As a consequence, ^{100}Mo samples need to be irradiated for short times, i.e. basically no longer than half-life ($T_{irr} \leq 6$ h) so that the N^{99gTc}/N^{99mTc} ratio in the final product may be considered still acceptable, compared to that provided by the current Mo/Tc generators [3].

In addition, it has to be noted that some interesting imaging *in-vivo* tests have also been performed by the Canadian group on healthy rats [5], to get a comparison between the generator-produced vs the cyclotron-produced ^{99m}Tc. The results have clearly shown that the labeling efficiencies, which potentially could be affected by the presence of large quantities of ^{99g}Tc, are instead well above the U.S. Pharmacopeia (USP) requirements (>90%).

Chapter 2

Aim of this thesis work: Target improvement

For direct production of ^{99m}Tc by cyclotron it is necessary to establish optimal irradiation conditions that involve the energy and the current of the beam, the target characteristics (purity, plate, recycle), and the irradiation time in order to obtain high yield and purity.

The feasibility of direct production of ^{99m}Tc by cyclotron was widely demonstrated in theoretical and experimental studies in literature, but some issues are still outstanding, such as the identification of the target capable to produce sufficient amounts of ^{99m}Tc for the clinical use.

Many research groups have developed different techniques to produce Mo target, however, the majority of them does not meet the requirements that a metallic Mo target for cyclotron production of Tc must follow:

- high heat dissipation level (good thermal conductivity);
- uniform and controlled thickness;
- high density;
- low level of oxidation.

INFN – LNL suggests an innovative approach to target development based on the deposition of thick ^{100}Mo film on a suitable substrate. This thesis intends to improve some aspects related to the magnetron sputtering technique deposition method.

2.1 State of art about the techniques for Mo target manufacturing

Several ways of preparing Mo targets for Tc production using the ^{100}Mo(p,2n)^{99m}Tc reaction have been studied. Target manufacturing methods are centered on different approaches: electrophoretic deposition; electroplating; press and sintering; rolling; brazing.

The majority of prepared targets have been studied during and after the irradiation in order to verify if they were adequate for the purpose (i.e.: resist to long time irradiation, dissipate heat quickly, low activation products).

2.1.1 Electrophoretic deposition

In Electrophoretic deposition, charged powder particles, dispersed or suspended in a liquid medium, are attracted and deposited onto a conductive substrate of opposite charge on application of a DC electric field [8].

Hanemaayer et al. 2014 have prepared Mo targets making use of electrophoretic approach to deposit the molybdenum metal on a tantalum metal surface followed by sintering at 1700 °C. This process produces a robust target that has been tested at 260 μA. The deposits were uniform and adherent but not suitable for high current beam [9].

2.1.2 Electrochemical methods: electrodeposition

In order to prepare a Mo target material for its irradiation with protons the preliminary studies on Mo electrodeposition on platinum support from aqueous solutions were performed by R. Mikolajczak et al. [6]. Aqueous electroplating was found to give coatings of low thickness, non-adherent to the backing or containing Mo-oxides. These features make the coatings unsuitable for further development as a stand-alone method for the target preparation.

Different electroplating bathes have been used for target support electroplating also by A.H. Al Rayyes [6]. The quality of the different electroplated Mo layer on copper substrate was not suitable for high current proton beam and high activity ^{99m}Tc production. The thickness obtained by different electroplating procedure do not exceed 2-3 micrometer having a total surface of 10 cm^2.

2.1.3 Powder sintering and pressing

Pressing and sintering methods are used to form solid parts from powders. Sintering is a heat treatment process by which metal powder compacts are transformed into coherent solids at

temperatures below their melting point. During sintering, the powder particles are bonded together by diffusion and other atomic transport mechanisms, and the resulting somewhat porous body acquires a certain mechanical strength.

Successful irradiations have been performed at some level using pressing and sintering technique, but the bulk sintering of the isotope powders results in a massive target that will not support high power density fluxes because of its intrinsic porosity between grain boundaries [6].

2.1.4 Rolling

^{99m}Tc production by 18 MeV protons on ^{100}Mo target has been evaluated by A. Salvini et al. [6] in collaboration with INFN – LNL (Legnaro National Laboratory) for the target preparation.

The tested target consists of few foils ^{100}Mo enriched of 25 μm stick together and separated by aluminum foils. The starting material is Mo powder enriched in ^{100}Mo (99,05%) compacted in pellet of 5 mm in diameter at high pressure. The pellet is molten by electron gun evaporator in order to obtain a metallic sphere. Then sphere was laminated by rollers until the desired thickness was obtained. This method allows to get uniform thickness (20%) and planar foil. The targets obtained by this technique were tested for the irradiation with energy of 18 MeV in order to test the separation methods proposed, but the thickness of 25 μm is not suitable for high current proton beam.

B. A. Thomas, J. S. Wilson, and K. Gagnon [10] have developed for ^{100}Mo target fabrication entails rolling ^{100}Mo powder into a foil of desired thickness, and then using diffusion bonding to bond the foil onto an aluminum backing plate. These results demonstrate a robust, relatively inexpensive target with desirable physical properties that can handle high irradiation currents during large scale production of ^{99m}Tc via the ^{100}Mo(p,2n)^{99m}Tc reaction. The only disadvantage was the burns marks on the surface after irradiation at 350 μA and 500 μA; the burn marks are attributed to areas of poor bonding between the ^{100}Mo foil and the aluminum back plate, which would cause poor thermal conductivity. In addition, the radionuclide purity could be affected by the contaminants from bonding.

2.1.5 Laser melting

BEST Cyclorons Inc. company has developed ^{100}Mo deposition by laser melting technique, but the uniformity was not enough and not good for the purpose.

2.1.6 Brazing of Target to the copper baseplate and the problem of a dirty interface

S.K. Zeislera et al. [11] have developed a novel system based on a pressed and sintered ^{100}Mo plate brazed onto a dispersion-strengthened copper backing. The pressed molybdenum plate is sintered and then brazed in a GCF1100 inert gas furnace at ~ 750 °C onto a backing manufactured from a dispersion strengthened copper composite using a high temperature silver-copper-phosphorus brazing filler. This process yields a mechanically and thermally robust target system for high beam power irradiation but there is the problem of a dirty interface because of the brazing filler that could be activated during irradiation and produce impurities (long lived radioisotopes) [11].

2.2 Proposal of an advanced target preparation

One of the most crucial issues for the success of the direct production of ^{99m}Tc by cyclotron consists in the target fabrication. Indeed, both the target itself and the target holder must have the peculiarity to dissipate heat power as much as possible.

Therefore, solid enriched molybdenum accelerator targets must be sufficiently thick, durable and heat conductive for irradiation at the required current and energy because the problem of heat removal from narrow irradiation area is crucial for the effectiveness of the nuclear reaction. Furthermore, targets must also be sufficiently durable to allow for transport post-irradiation and the post irradiation process should produce as few impurities as possible (i.e. chemical inertness of the backing plate).

The poor thermal conductivity of molybdenum oxide severely limits the amount of beam current that can be applied to these targets and it would appear that only metallic Mo

targets will be amenable to the high power irradiations needed for the large-scale production of ^{99m}Tc [12].

2.2.1 Magnetron sputtering as a solution (clean and mass production)

Several strategies for metallic molybdenum deposition have been tested (see section 2.1), including sintering and electroplating but further development towards other methods is necessary.
INFN - LNL proposes the fabrication of thick Molybdenum films by magnetron sputtering technique.

2.2.2 The advantage of producing thick films by magnetron sputtering

Magnetron sputtering has emerged to complement other vacuum coating techniques such as thermal evaporation and electron-beam evaporation. However, these techniques show certain disadvantages. In particular, alloys and refractory metals cause problems because of differences in alloy constituent vapor pressures and their high melting points. In addition, compounds can dissociate into their chemical constituents at the low evaporation pressures used.

Magnetron sputtering overcomes these problems and has got many other advantages. The primary advantages are:

- ✓ high deposition rates,
- ✓ ease of sputtering any metal, alloy or compound,
- ✓ high-purity films,
- ✓ extremely high adhesion of films to substrate,
- ✓ excellent coverage of steps and small features,
- ✓ ability to coat heat-sensitive substrates,
- ✓ ease of automation,
- ✓ excellent uniformity on large-area substrates [13].

Nevertheless, the maximum thickness of sputtered films does not overcome a few microns; therefore, for the deposition of thick Mo film, suitable for target fabrication, the idea is to deposit films of a few tenths of microns by the stress relaxation technique.

2.2.3 Treatment of the target after irradiation (target processing)

After the production of ^{99m}Tc via the ^{100}Mo(p,2n)^{99m}Tc reaction, a separation procedure should be always accomplished to separate ^{99m}Tc from bulk ^{100}Mo and isolate the radionuclide of interest under a suitable chemical form.

Because of their *in vivo* application, medical radionuclides are usually supplied in aqueous solutions that *must* comply with stringent quality standards according to Pharmacopeia requirements. Specifically, the characteristics of high radionuclidic and chemical purity are considered mandatory. These requirements can be fulfilled by developing efficient separation procedures that yield the radionuclide in an ultrapure form within a relatively short time to prevent excessive loss of radioactivity through its natural decay. For these reasons the procedures must be automatic and they should be performed as brief as possible.

Various physico-chemical separation methods have been proposed since different target materials (e.g. Mo metal, MoO_3, etc.) were used for irradiation by different groups.

The separation of ^{99m}Tc target follows procedures established by several authors based on the target dissolution in H_2O_2 at elevated temperature.

Then the solvent extraction occurs by using resins or acidic and basic alumina (e.g. Chattopadhyay, MEK, ABECTM) to separate the ^{99m}Tc from other impurities formed during irradiation [12].

Therefore, several ^{100}Mo target design considerations are required, in addition to molybdenum deposition technique, including the selection of target backing material, concerning:

- thermal properties;
- machinability;
- mechanical strength;
- chemical inertness;
- activation products;
- cost.

2.2.4 Problem of backing plate chemical resistance

The target back plate supporting the ^{100}Mo must be chemically inert to target dissolution conditions but, ideally, it should also be able to dissipate high thermal loads of irradiation, not contaminate target substrate with radionuclidic by-products, and be adequately inexpensive to allow for single use [10].

The most common material used as backing plate is copper [14], for its good thermal conductivity (390 W/(m K)) and its relatively low cost.

However, copper is highly activated under the proton beam during irradiation producing a huge amount of long-lived radio-impurities and, also, it dissolves in H_2O_2. These drawbacks mean further separation modules in order to obtain the purity of the final product, intolerable with the necessity to shorten and automatize the procedures.

Gold could be used as backing plate but its thermal conductivity is lower than copper and it is very expensive.

Therefore, the choice of better material mainly depends on the strategy followed for the chemical dissolution of Mo irradiated sample as well and on the technique for the molybdenum deposition on the support material.

2.2.5 Sapphire and DLC as a solution

The proposal of LNL is to use a thin layer of ceramic material that is inert chemically and under the beam, avoiding radioisotope impurities. Further, both the target itself and the target holder must have the capability of being irradiated at high beam current, and so, the peculiarity to dissipate as much as possible the power heat level. Sapphire and CVD diamond substrates metalized and brazed to the target holder case (Diamond like carbon, DLC) could be a solution. The first one has the highest thermal conductivity between all ceramic materials.

DLC is a class of amorphous carbon material that displays some of the typical properties of diamond. One of many remarkable properties of diamond is its unsurpassed thermal conductivity. With a value of 2000 W/(m K) it exceeds that of copper by a factor of five. In contrast to metals, where electrons conduct heat, lattice vibrations are responsible for diamond high thermal conductivity.

2.2.6 Problem of deposition technique

The proposal of the advanced target preparation consists in a ~100 μm thick of ^{100}Mo deposited by magnetron sputtering on sapphire or DLC.

The choice of magnetron sputtering as deposition technique is justified by the fact that it is the suitable methods that allows depositing films on ceramic substrate resulting uniform, dense and adherent.

The only drawback to be solved is the elimination of residual stress of sputtered-film, because high residual stress can cause plastic deformation (buckling or bending), cracking in the deposit or the substrate, or cracking at the substrate-deposit interface.

Therefore, stress must be avoided in order to respect the requirements for Mo target for cyclotron production of ^{99m}Tc.

The next section is devoted to magnetron sputtering and the methods to reduce stress during sputter deposition.

Chapter 3

Magnetron sputtering as deposition technique

3.1 What is magnetron sputtering?

Sputter deposition is a widely used technique in order to deposit thin films on substrates.
In sputter deposition, material is made to go into the vapor phase by the physical interaction of particles impacting the source material (also referred to as “target”).

In sputtering, the target material and the substrate are placed in a vacuum chamber in order to avoid oxygen and collisions with gas molecules during the transport of evaporant from the source to the substrate.

A voltage is applied between target and substrate so that the target is the cathode and the substrate is attached to the anode. A plasma is created by ionizing a sputtering gas (generally a chemically inert, heavy gas like Argon) that bombards the target and sputters off the material to be deposited.

The process begins with a stray electron near the cathode that is accelerated towards the anode and collides with a neutral gas atom converting it to a positively charged ion (Figure 9).

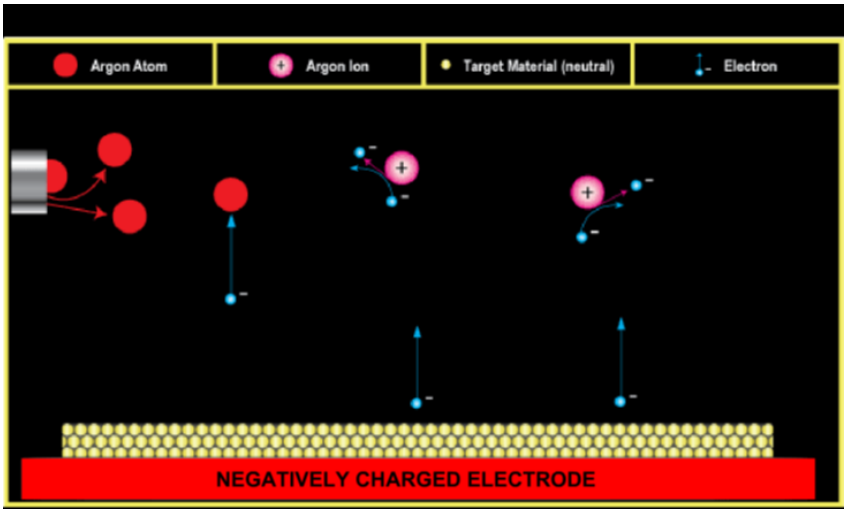

Figure 9 The beginning of the sputtering process.

The process results in two electrons, which can then collide with other gas atoms and ionize them creating a cascading process until the gas breaks down. The breakdown voltage depends on the pressure in the chamber and the distance between the anode and the cathode. At too low pressures, there are not enough collisions between atoms and electrons to sustain a plasma. At too high pressures, there are so many collisions that electrons do not have enough time to gather energy between collisions to be able to ionize the atoms.

When ions collide with surface atoms on the target, the energy transfer can knock some of these atoms off the surface. Sputtered atoms from the target make their way onto the substrate through diffusion (Figure 10).

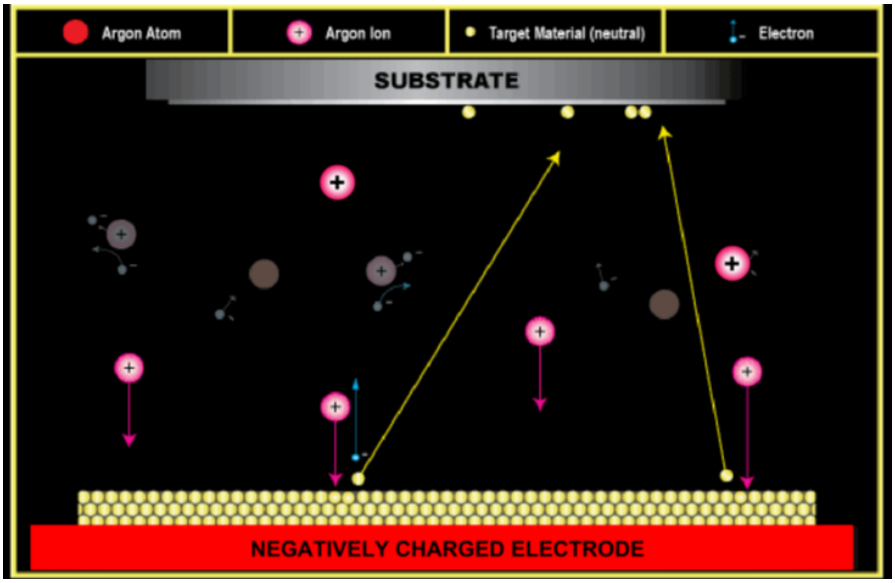

Figure 10 Deposition of target material during sputtering process.

There is a wide variety of sputtering techniques that are currently used to deposit thin films: diode sputtering, RF sputtering, ion beam sputtering and magnetron sputtering [15]. In this section magnetron sputtering will be described.

Magnetron sputtering makes use of magnetic field to constrain the plasma close to the sputtering target. Magnets situated underneath the target cathode constrain the electrons emitted from the cathode to orbit in close proximity of the cathode as showed in Figure 11.

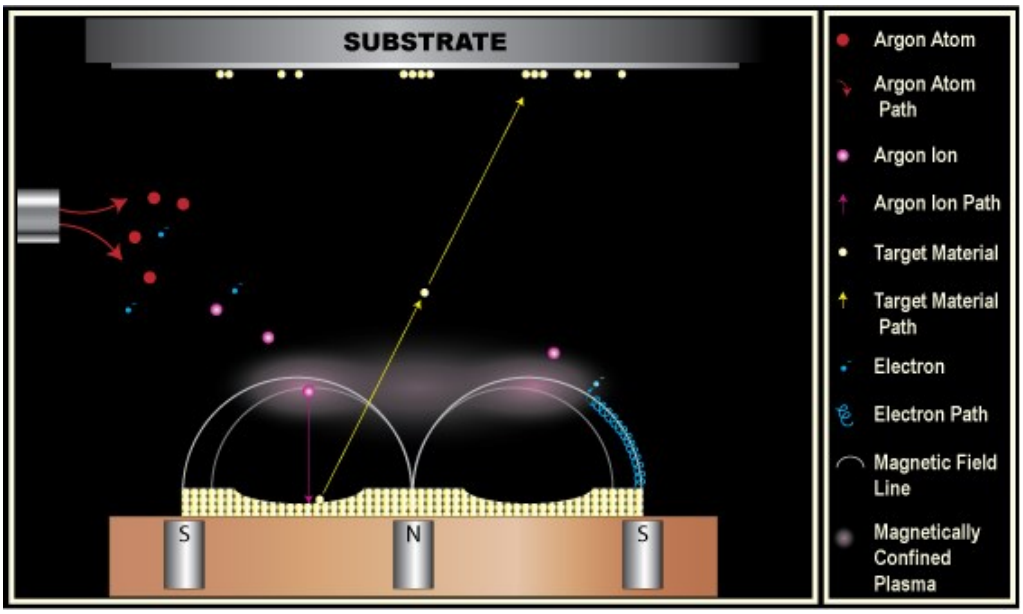

Figure 11 Magnetron sputterign deposition: magnets under the target confine the plasma close to the target.

As the electron trajectory is elongated, the probability that such an orbiting electron will strike a process gas molecule, causing an ionization, is greatly increased without the need to increase gas pressure. In this way, the ions can reach the cathode with almost full discharge voltage and the sputtered atoms can reach the substrate with only a few collisions. Also, the deposition rate, a technically meaningful criterion, will dramatically increase compared to simple diode glow discharge systems [15].

The strength of the magnetic fields and placement of the magnets with respect to the cathode is crucial to the proper operation of a magnetron sputter deposition source.

In Figure 12 different magnets configuration and the consequent plasma confinement are shown. Type-II unbalanced Magnetron will be explain deeper in the next section (4.2).

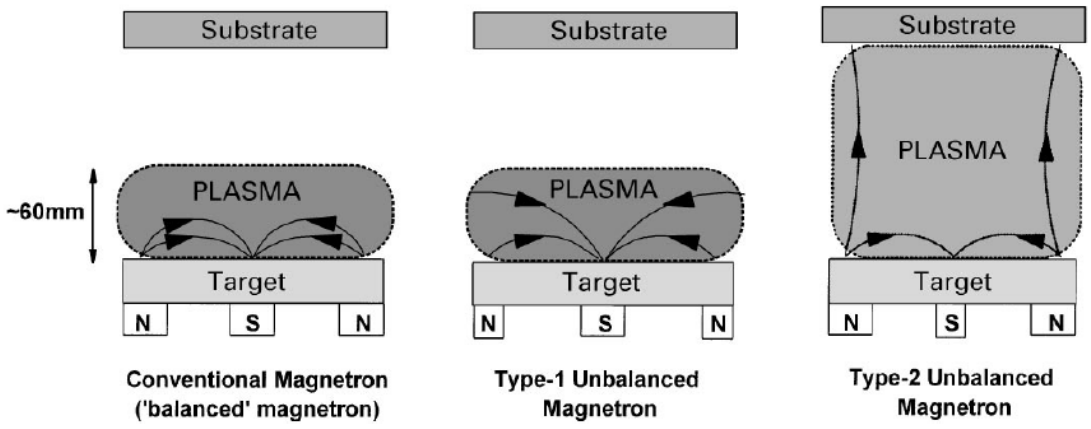

Figure 12 Schematic representation of the plasma confinement observed in conventional and unbalanced magnetrons [15].

Magnetron sputtering technique allows depositing thin films having the required physical and chemical proprieties thanks to the possibility to control the parameters that influence the growth of the desired film:

- argon pressure;
- sputter voltage;
- substrate bias voltage;
- substrate temperature;
- particle energy.

By varying these parameters one can generate thin films of a given material that have different mechanical strength, adhesion, optical reflectivity, electrical resistivity, magnetic properties and density.

3.2 Control of stress in magnetron sputtering

Materials synthesized by deposition techniques are often plagued by high levels of residual stress as a result of film growth and constraints imposed by their substrates.

In this section, it will be described what stress is and how the stress could be controlled according to a number of studies focused on experimental, theoretical and computational approaches [16], [16]–[21].

3.2.1 What is stress

A piece of solid is under stress when its atoms are displaced from their equilibrium positions by a force. The displacement is governed by the interatomic potential. It is well known that the potential Φ and the internal force F (F $=-\partial\Phi/\partial r$) between two atoms, as a function of interatomic distance, generally obey the schematic relations shown in Figure 13 a)**.**

When an external force is applied, it is defined:

$$F_{ex} = +\frac{\partial \Phi}{\partial r}$$

Where the sign is positive compared to the internal force between two atoms. An external tensile force tends to lengthen the solid and in turn to increase the interatomic distance. Based on the sign convention, a force that increases the interatomic distance is positive, and hence the tensile force (or stress) is positive. An external compressive force (or stress) which tends to shorten the solid is negative. The interatomic potential, the external force, and the sign of the force are shown in Figure 13 a), b) and c) respectively.

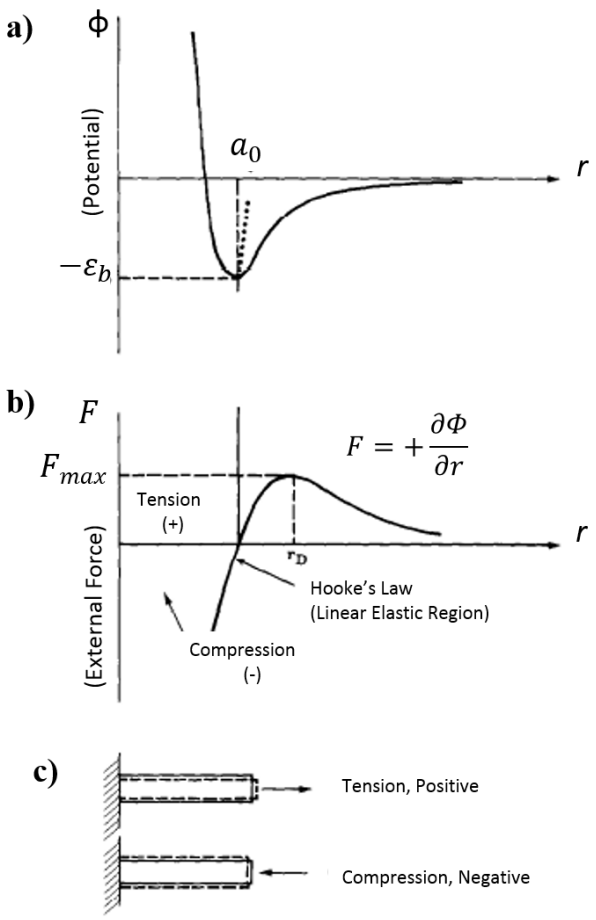

Figure 13 (a) interatomic potential function plotted against interatomic distance. The dotted curves shows the anharmonicity of atomic vibration; (b) Applied force plotted against atomic displacement; (c) The direction and sign of applied force by convention [22].

Thin films are stressed even without the application of external loading and are said to possess internal or residual stresses [23].

3.2.1.1 Types of stress

Residual stresses in deposited films are of two origins. The first kind arises from the imperfections built in during growth (the so-called growth stresses).

The other source of residual stress is due to the mismatch in the thermal expansion coefficient between the substrate and the deposited material. Its magnitude and size depend on the values of the thermal expansion coefficients as well as the thickness and size of the substrate and deposit [23].

More recent investigations[16], [16]–[21], [23] are directed at understanding the fundamental, atomic-level mechanism of stress generation.

Compressive stress results when heavy ions or energetic particles strike the film during deposition causing atomic displacement and densification above these expected in equilibrium [17], [21], [24]. Therefore, films under compression will try to expand, and if the substrate is thin, the film will bow the substrate with the film being on convex side (Figure 14).

Tensile stress is usually explained by a grain coalescence mechanism, where neighboring grains of the growing film are presumed to spontaneously join under the action of interatomic forces, eliminating microvoids surrounding the columnar grains. This net in-plane contraction produces tensile stress in the growing film [25]. Therefore, the films under tensile stress will try to contract bowing the substrate so the film is on the concave side (Figure 14).

The tensile stress should increase with a decrease in grain size and/or an increase in the difference between surface and grain boundary energies. Also, surface roughness, was correlated with the observed tensile trend during film growth, suggesting that a smooth surface may be required to maintain low levels of stress [17], [21], [25].

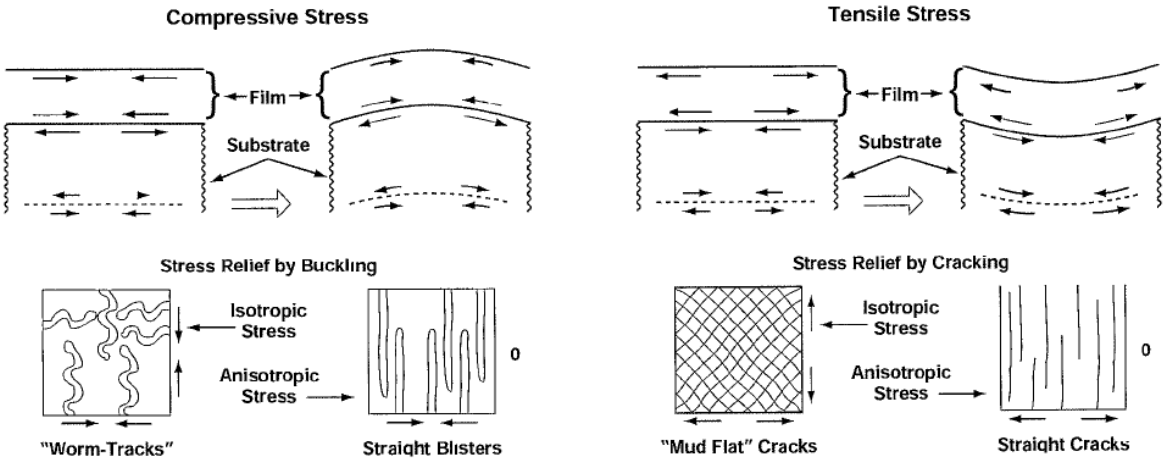

Figure 14 Deformation and Fracture in stressed film [17].

3.2.1.2 Problem for films

High residual stresses can cause plastic deformation (buckling or bending), cracking in the deposit or the substrate, or cracking at the substrate–deposit interface, adhesion problems, posing serious practical problems [25].

In particular, for the purpose of this thesis it is mandatory to avoid stressed films because poor adhesion between Mo films and substrate influences thermal conductivity, one of the most important requirements for cyclotron target. Reduction of stress is therefore an important technological issue.

3.2.1.3 Increase with the thickness

While thin films may be adequately characterized by an average stress value, thick films require more detailed measurements. The total stress increases with the thickness, and the stresses may not be uniform through the film thickness (i.e. a stress gradient in the deposit) if the growth mode and film density change with thickness and/or if some region has been annealed more than others during the deposition process [17], [25].

3.2.2 Parameters influencing stress

Stress state in deposited films is caused by mechanisms depending on the energy supplied to the growing film surface. Magnetron sputtering technique allows to control the kinetic energy of the particles in order to minimize stress. The variables, which significantly involved the change of kinetic energy, and so the microstructure growth, are sputtering gas pressure, temperature of the holder, bias, etc.

3.2.2.1 Microstructure

Intrinsic stress is a sensitive function of film microstructure created in the film as atoms are deposited on the substrate.

The microstructure of magnetron sputter-deposited films is defined by the identity of the particles arriving at the substrate, their fluxes, and the energy per particle that influences the growth of the film.

The steps in the growth of thin films are generally referred to as nucleation and growth.

In nucleation, the atoms and molecules, which are arriving (called adatoms) at the surface lose thermal energy, and the surface absorbs that energy. Depending on the amount of thermal energy the adatoms and the surface have, the adatoms move about on the surface until they lose the thermal energy required to move about the surface (referred to as adatom mobility). As nuclei continue to form, the film grows into a continuous sheet covering the substrate.

Chemical interactions between the adatoms and the surface determine the strength of the bond between the film and substrate.

Once a few monolayers of evaporant have condensed on the substrate, the film continues to grow in thickness as if the entire substrate were made of the deposited material. During film growth the microstructure of the deposited film will be developed.

This microstructure could be described in terms of grain size, orientation, porosity, impurity content, and entrained gases.

Intrinsic stress results from the microstructure created in the film as atoms are deposited on the substrate; therefore, the microstructure and morphology of thick single-phase films have been extensively studied for a wide variety of metals, alloys, and refractory compounds [25].

Structure zone models (SZMs) have long been used as a convenient means of displaying the relationships between process parameters and the structures and, therefore the properties of PVD coatings [15], [23].

The structural model was first proposed by Movchan and Demchishin, and was subsequently modified by Thornton [26] as shown in Figure 15 a) and b) respectively [23].

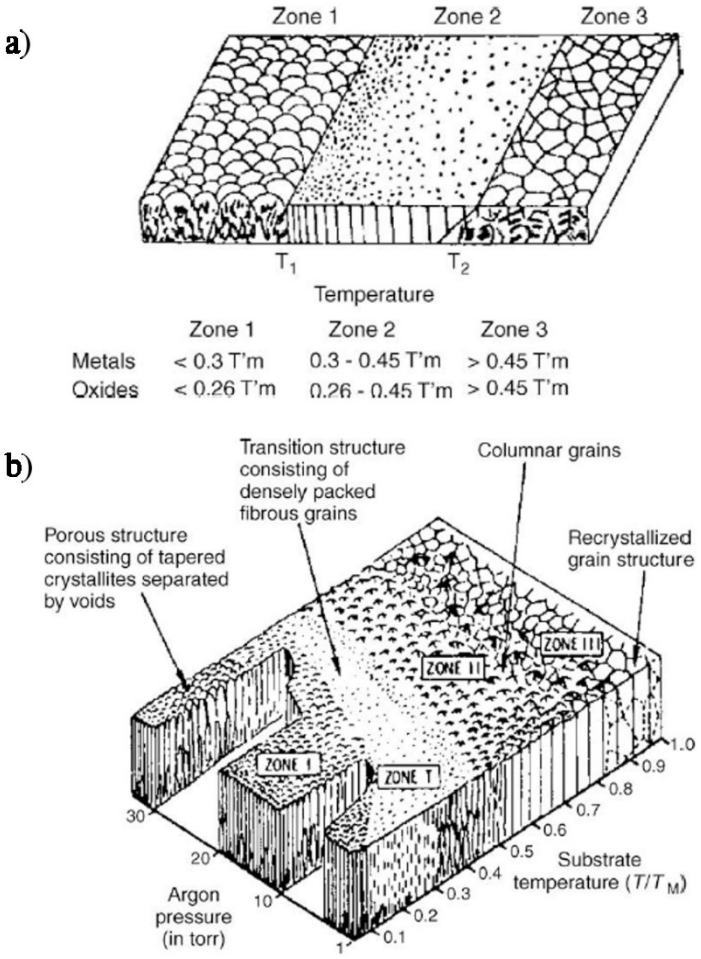

Figure 15 a) Structural zone in condensates; b) Thornton structural zone model [23].

The revised SZM [27] (Figure 16) proposes a graphic representation of physical process occurring at atomic level when the following sputtering parameters change:

- process gas pressure;
- ratio T/T_m where T is the substrate temperature, and T_m is the melting temperature of the deposited material;
- substrate polarization by applying voltage V_s.

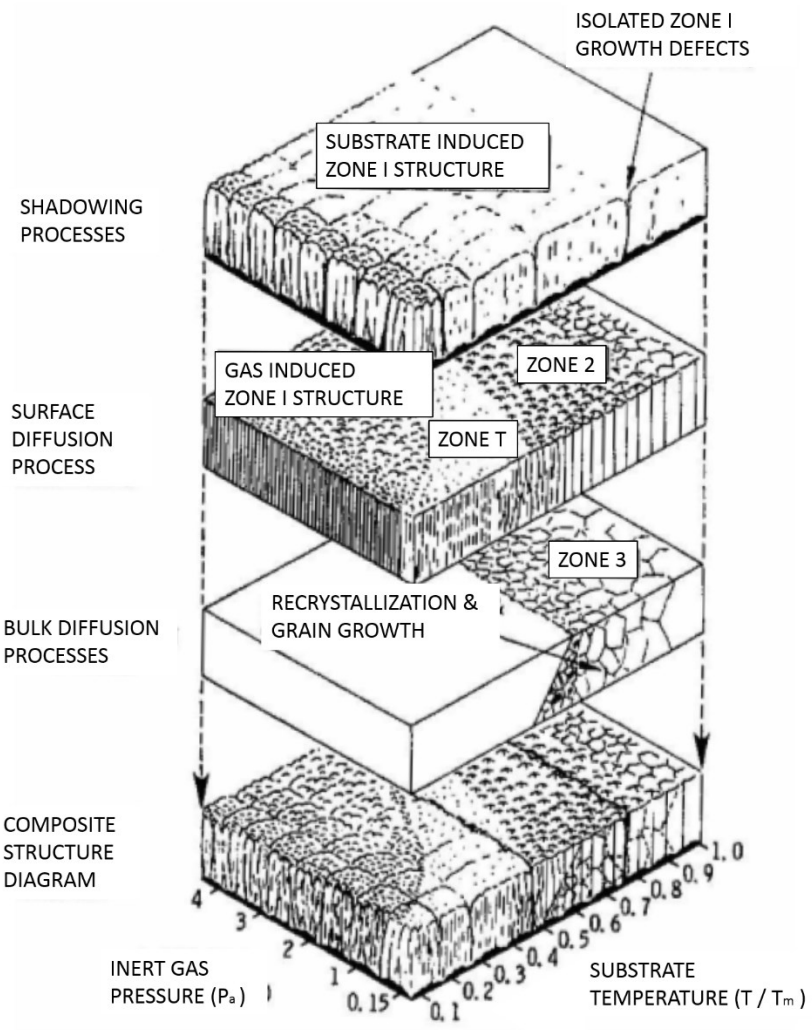

Figure 16 Schematic representation of sputtered-film structures showing the superimposition of shadowing, surface-diffusion, and bulk-diffusion process that establish structural zones.

3.2.2.2 Sputtering gas pressure

Internal stresses in refractory-metal films prepared by magnetron sputter deposition strongly depend on the working-gas pressure.

A general feature is the transition pressure below which the films are in compression, whereas above this pressure the films have tensile stress. Such stress reversals are dependent on energetic bombardment by reflected neutrals and/or sputtered atoms. The working-gas pressure is expected to moderate the flux and energy of these particles.

At relatively low pressures, the arriving atoms have high kinetic energy and the resulting film has a dense microstructure (Figure 16), experiencing compressive stress. This compressive

stress is explained by atomic peening caused by the impact of energetic particles (reflected neutrals/sputtered atoms).

At relatively high pressures, the frequency of gas phase collisions increases, reducing kinetic energy of sputtered neutral atoms and reflected neutrals bombarding the growing film exhibiting an open porous microstructure. Interatomic attractive forces produce tensile stress [21], [24].

The grain size does not appear to change with the increasing pressure but the grain morphology changes dramatically (increase of surface roughness) [25].

The rapid change of stress with pressure allows only a narrow window of pressures that yields reasonably low-stress value. Therefore, obtaining low-stress films by controlling only the working-gas pressure is not a robust method [20].

3.2.2.3 Difference of thermal expansion coefficients of film material and substrate

Thermal-mismatch stress is the most common source of extrinsic stress.
When a thin film is deposited on a thick substrate at elevated temperature, and subsequently cooled and operated at ambient temperature, the difference between the thermal expansion coefficients of the film and substrate creates stress and strain. The growth of the film does not allow adatoms to condense in their least energetic association with one another [20].

The thermal expansion coefficient is an intrinsic property of a pure element, and it is defined as

$$\alpha = \frac{d\varepsilon}{dT}$$

Assuming that the thermal expansion coefficients are temperature independent, the strain caused by thermal expansion is then simplified:

$$\varepsilon(T) = \varepsilon(T_0) + \alpha \cdot \Delta T$$

where the first part of the equation is assumed to be negligible and the last part, the strain caused by thermal expansion.
As the substrate is very thick in comparison to the film, it can be assumed, that the substrate contracts to the size, it would have attained in absence of the film. With this assumption, we can write the strain of the substrate as

$$\varepsilon_s = -\alpha_s \cdot \Delta T$$

Where α_s represents the coefficient of thermal expansion for the substrate and the minus sign, the compression of the film. The film then gets this same strain due to the fact, that it is attached to the substrate.

$$\varepsilon_{f,attached} = -\alpha_s \cdot \Delta T$$

If the film were unattached, however, its strain would be

$$\varepsilon_{f,free} = -\alpha_f \cdot \Delta T$$

Where α_f represents the coefficient of thermal expansion for the thin film.

The difference between the strains film features with and without attachment to the substrate is the thermal mismatch strain

$$\varepsilon_{f,mismatch} = \varepsilon_{f,attached} - \varepsilon_{f,free} = (\alpha_f - \alpha_s) \cdot \Delta T$$

The thermal mismatch leads to stress in the film. From previous equation, we can write in case of biaxial system

$$\sigma_{f,mismatch} = \frac{E}{1-\nu}(\alpha_f - \alpha_s) \cdot \Delta T.$$

By convention, tensile stress is positive, compressive stress is negative. Therefore, if $\alpha_f < \alpha_s$ a compressive stress will be expected and if $\alpha_f > \alpha_s$, a tensile stress will appear.

Films containing internal tensile stresses bend the substrate concave upward. Similarly, compressive stresses lead their origin from films that tend to initially expand relative to the substrate as shown in the following Figure 17 [28].

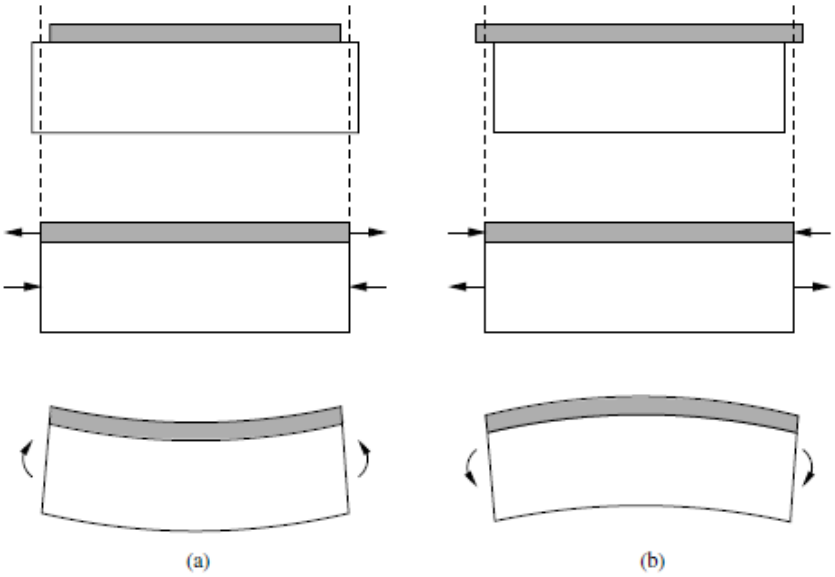

Figure 17 Sequence of events leading to a) residual tensile stress film; b) residual compressive stress in film.

3.2.2.4 Temperature of the holder

In SZMs the homologous temperature, T/T_m, of the coating is used to describe the thermally induced mobility of the coating atoms, a variable that influences the bombardment of the growing film by energetic particles.

The temperature of the holder influences the implant of atoms to the film surface and therefore associated stress.

A reduction in stress by movement of the implanted atoms to the film surface is energetically favored, indeed, an increase in substrate temperature during sputter deposition corresponds to a negligible "thermally induced" stress value [20]. Instead, at substrate temperatures less than 20% of the melting point, intrinsic stress due to incomplete structural ordering dominates [24].

The mechanism could be explained as follow.

At low temperatures, the surface mobility of the adatoms is reduced and the structure grows as crystallites from a limited number of nuclei. It is not a full-density structure but contains longitudinal porosity of the order of a few hundred angstroms' width between the crystallites. It also contains a high dislocation density and has a high level of residual tensile stress. Such a structure has also been called 'Botryoidal' and corresponds to zone 1 in Figure 15 and Figure 16 [23].

As the substrate temperature increases, the surface mobility increases and the structural morphology first transforms to that of zone T, i.e. tightly packed fibrous grains with weak grain boundaries, and then to a full-density columnar morphology corresponding to zone 2 (Figure 16). The size of the columnar grains increases as the condensation temperature increases. Finally, at still higher temperatures, the structure shows an equiaxed grain morphology (zone 3) [23]. Therefore, at high T/T_m the densification of the film is accompanied by generation of a compressive growth stress after formation of a continuous film.

3.2.2.5 Distance target-substrate

Source to substrate distance influences thickness uniformity.

The number of collisions between the argon ions, electrons and material atoms could be approximated as $N = \frac{L}{\lambda}$ (where L is target-to-substrate distance and λ is pressure-dependent

mean free path) that is strictly correlated to the energy with which the adatoms deposit on the substrate [25].

The higher the distance, more collisions that create randomization on the sputtered film depositing on the substrate and ultimately better uniformity. However, the drawback to this is that the higher the distance, the lower the sputtering rates will be, and the tensile stress could increase because of low energy.

3.2.2.6 More energetic deposition

Stress control is achieved by varying the degree of energetic particle bombardment during sputtering [24], thereby there are some devices involving the change of kinetic energy: biasing of the substrate, high power impulse magnetron sputtering (HiPIMS), pulsed laser deposition (PLD).

Some processes use **biasing**. Biasing is the application of a voltage to the substrate such that surface bombardment by positive ions occurs on the substrate as well as on the target cathode. This causes re-sputtering of the depositing layer or at least an increase in surface energy. These effects also control film growth and improve step coverage profile and can eliminate some commonly observed defects such as microcrack formation [13].

Increasing bias voltages will lead to an effect similar to that of reduction of process gas pressure that is increasing the adatom mobility, resulting in better films in terms of microstructure. An RF-substrate biasing technique has been shown to improve the stress control over an optimum regime of cathode current, pressure, and the RF-substrate bias values [20].

Ionizing the sputtered vapor improves film quality, therefore many researches [29], [30] have studied physical vapor deposition techniques that provide substantial ionization of the sputtered material, produce high-quality coatings like high power impulse magnetron sputtering (HiPIMS) and Pulsed laser deposition (PLD).

The **HiPIMS** discharge generates large quantities of highly energetic ions thanks to very high pulse power densities with, in some cases, a directed flux of charged species. An increase in the ion flux greatly reduces intra-columnar as well as inter-columnar porosity, resulting in a dense and uniform film, with low level of tensile stress. However, several groups report on a significantly lower deposition rate for HiPIMS as compared to dc magnetron sputtering [29].

With the **PLD** method (Figure 18), thin films are prepared by the ablation of one or more targets illuminated by a focused pulsed-laser beam. During PLD, it is possible to tune the

film properties (stress, texture, reactivity, magnetic properties) by varying the kinetic energy of the deposited particles by changing different parameters (e.g., laser parameters such as laser fluence, wavelength, pulse duration and repetition rate; target-to-substrate distance, substrate temperature, background gas and pressure, which all influence the film growth).

The PLD technique is also flexible, because the spot size of the focused laser beam is small and, therefore, the target area may even be less than one cm^2. This allows to prepare complex samples with enrichments of isotopes or isotopic markers within the deposited film and for application when the sample is extremely expensive [30].

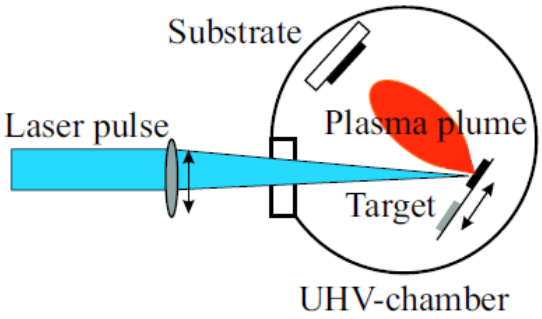

Figure 18 Schematic diagram of a typical laser deposition set-up.

3.2.2.7 Methods to reduce stress

The control of stress in physical vapor deposited films is of continued interest because of its close relationship to technologically important material property, adhesion strength to the substrate, the limit of film thickness without cracking, buckling or delamination.

During heating or cooling, very high stresses are induced in the coating when the thermal-expansion coefficients of the films and the substrate vary significantly from each other. Some of the methods to reduce the mismatch of thermal expansion coefficients include roughening of the surface for mechanical interlocking and the use of chemically compatible interlayers having intermediate expansion coefficients. These methods to enhance adhesion have been successful in some material systems; however, in very large thermal-mismatched systems, cracking or de-bonding of the coating can still occur.

Karabacak et al. 2005 [20] were able to significantly reduce stress values in sputter deposited tungsten films on Si surfaces by means of nanostructured layer by high working gas pressures that acts as a compliant layer under the subsequently deposited continuous film grown

under low gas pressure. In this way, they have obtained adhesion improvement and high critical thickness. Interestingly, the stress of multilayer film decreases as the total thickness increases. The incorporation of each additional nanostructure compliant layer (NCL) seems to increase the efficiency of compliance in the multilayer film. Therefore, NCL allows fabricating very thick films with reasonable low stresses.

Therefore, in the multilayer film deposition, every time a new layer is started, new, isolated crystals are nucleated on the previous layer (renucleation); in this case, there is a small stress associated with the beginning of each layer, as there is for deposition on a fresh substrate. It is therefore quite possible to have renucleation of each layer in the fabrication of the multilayers. By tailoring the precise thickness of the individual layers, it is possible to produce multilayered films with any average stress between wide limits (compressive to tensile) [16].

3.3 So what is the aim?

This thesis is set in the framework of LARAMED project at LNL and deals with the development of innovative target for production of ^{99m}Tc cyclotron-based, with the aim to deposit thick, adherent, dense and stress-free Mo film on appropriate substrate by magnetron sputtering technique.

This deposition method is simply and advantageous for thin film preparation, however thick films could be deposited optimizing magnetron sputtering parameters, and using the strategy of multilayer deposition.

This thesis demonstrates a method to obtain a good Mo film, of a suitable thickness, by optimizing some deposition parameters that influence residual stress in thick films achieving the best recipe.

In particular, working gas pressure and temperature of the holder were taken into account as parameters that control stress in film deposition.

Another important problem is the suitable choice of the backing material. This thesis proposes the use of high chemical resistant material, like sapphire.
Since sapphire has high brittleness, the task of the deposition of Mo onto this type of substrate is making control of stress inside the deposited film an even more critical challenge.

Chapter 4

Experimental methods and equipment

4.1 Four chambers sputtering machine

The sputtering system consisted of four vacuum chambers connected through the central zone and separated by pneumatic gates in order to be able to carry on processes in different chambers in series (Figure 19). Deposition was carried out in a cylindrical, stainless steel vacuum chamber of 25 cm in diameter and 25 cm in length (Figure 20). Base pressure of $5 \cdot 10^{-6}$ mbar could be reached without backing out by means of Pfeiffer turbo molecular pump of 360 l/min and Varian Tri Scroll Pump 210 l/min as a primary pump, but system also allowed baking for improving of vacuum.

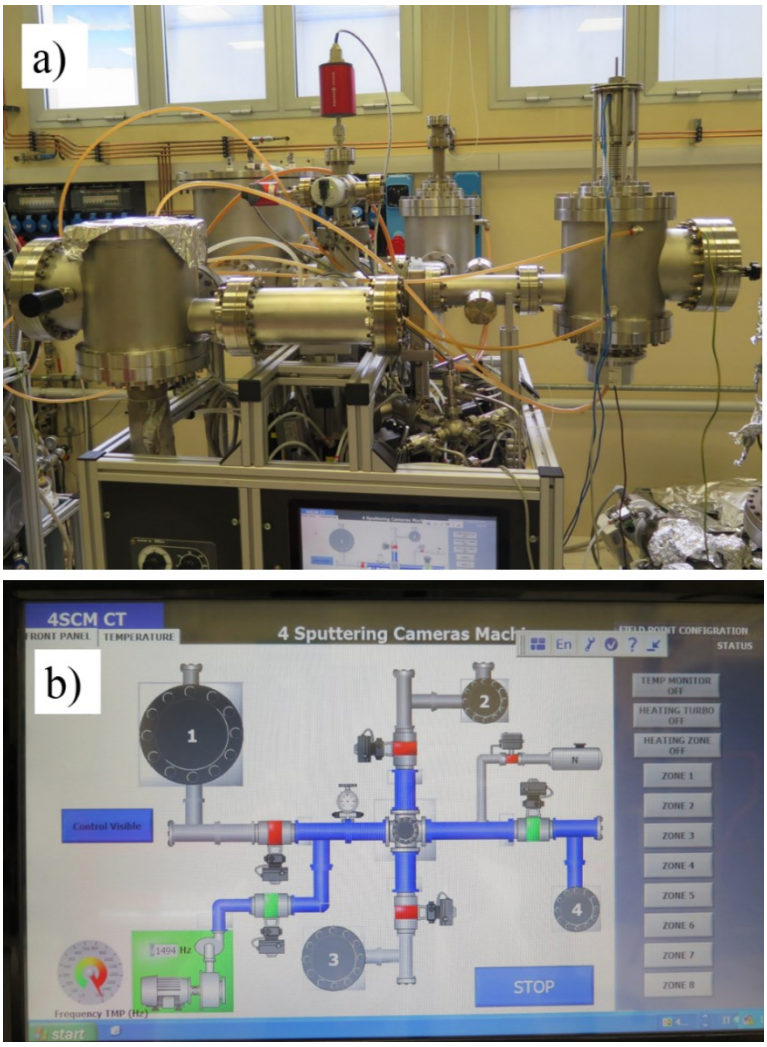

Figure 19 (a) 4 chambers sputtering system; (b) control panel.

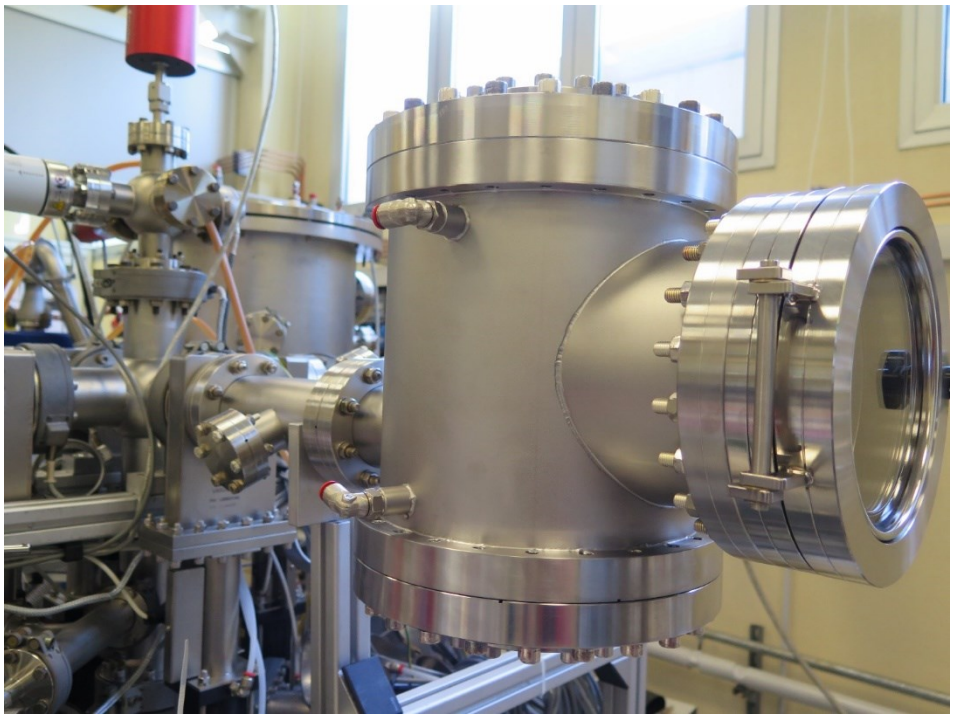

Figure 20 Chamber used to carry out the experiments.

4.2 Standard magnetron (unbalanced II type)

The deposition was performed by the 2 inches in diameter planar unbalanced magnetron cathode source of the II type (Figure 21) with low level of unbalancement in the Window and Savvides classification [31].

Figure 21 2 inches planar unbalanced magnetron.

In II type UBM the outer ring of magnets is strengthened relative to the central pole. Not all the field lines are closed between the central and outer poles in the magnetron: some are directed towards the substrate. Consequently, the plasma is no strongly confined to the target region, but is also allowed to flow out in the substrate direction as shown in Figure 22, UBM is characterized by higher ion and electron flux than conventional balanced magnetron.

In II type unbalanced magnetron, a central plasma plume is trapped in a secondary confinement. A plasma washing action will remove impurities weakly bounded to the growing film, increasing the film purity and densifying the structure.

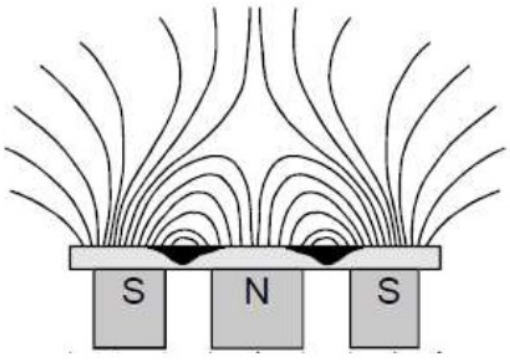

Figure 22 Schematic representation of the plasma confinement observed in unbalanced magnetrons Type-II.

4.3 Choice of Substrate-Target distance

In order to provide coating uniformity onto substrates, the depositions were carried out with a distance of 6 cm between target and substrates (Figure 23).

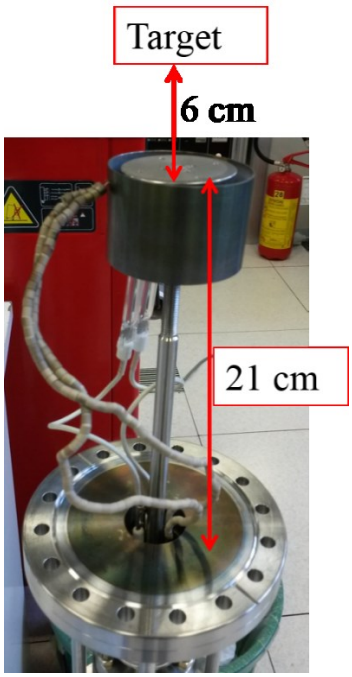

Figure 23 Target-substrates distance.

4.4 Substrate holders

Depositions were performed onto different planar substrate holders with the possibility to cool down or to heat up the substrate keeping constant distance to the cathode 6 cm (Figure 24).

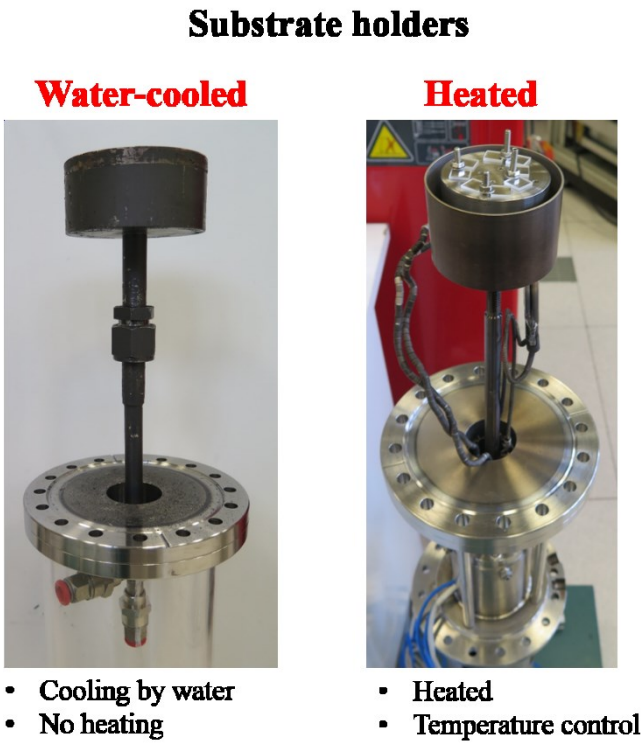

Figure 24 Substrate holders used and their characteristics.

The heating of the sample holder is performed by an infrared lamp connected to a transformer. A tension regulator, controlled manually, was used in order to heat up and cool down slowly. A thermocouple placed inside the target holder plate was used to read the temperature. The Figure 25 shows the devices used to heat the substrate holder.

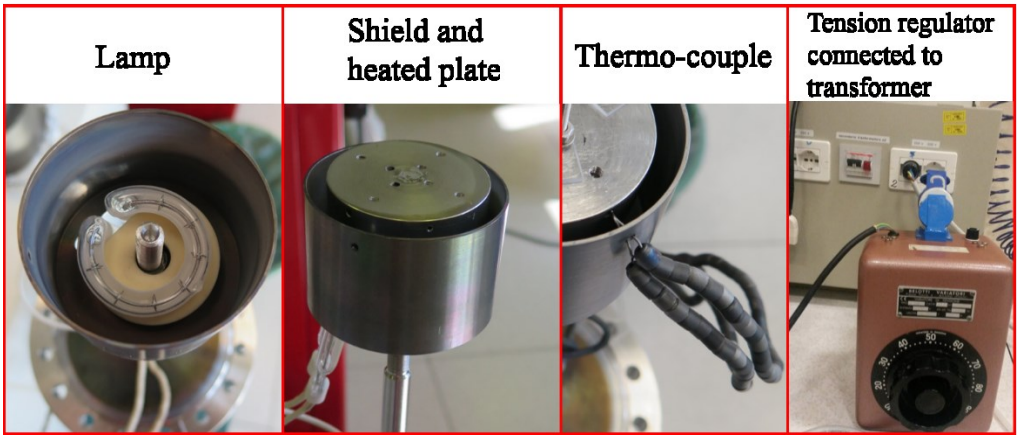

Figure 25 Devices needed to heat the substrate holder.

4.5 Materials used

4.5.1 Target

A high-grade bulk Nb for superconducting cavities (99.99% purity, RRR=250) has been used as a target for sputtering parameter optimization.

Natural molybdenum 99.99% purity, purchased by MaTeck GmbH, was used for sputtering deposition.

4.5.2 Substrate

Materials used as substrate were Quartz, Sapphire and Copper.
Quartz pieces 9 x 9 x 1 mm were purchased from Helio Italquartz.
Copper coins with a diameter of 13 mm and 0,5 mm thickness were cut in LNL mechanical workshop by electroerosion.
Sapphire pieces 10 x 10 x 1 mm and sapphire coins with diameter of 13 mm and thickness of 0,5 mm were purchased from Meller Optics, Inc. The sapphire coins are exactly IR grade single crystal sapphire, with Random and C-axis orientation.

The samples are shown in Figure 26.

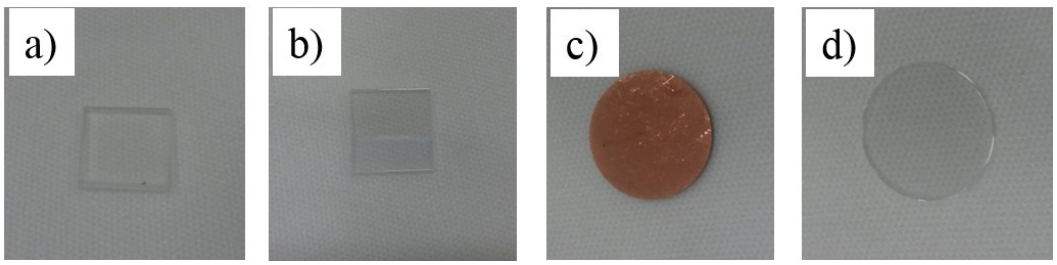

Figure 26 a) quartz; b) sapphire; c) copper coin; d) sapphire coin (diameter 13 mm, thickness 0,5 mm).

In the following table (Table 2) the thermal features of each material are shown.

Table 2 Thermal features of materials.

	Thermal expansion coefficient	Thermal conductivity	Melting temperature
Substrate materials			
Quartz	0,6 x 10^{-6} / °C	8 W/(m K)	~ 1000 °C
Sapphire	6 x 10^{-6} / K	40 W/(m °C)	2030 °C
Copper	17 x 10^{-6} / °C	390 W/(m K)	1084 °C
Target materials			
Molybdenum	4,8 x 10^{-6} / K	138 W/(m K)	2623 °C
Niobium	7,31 x 10^{-6} / °C	53,7 W/(m K)	2477 °C

4.5.3 Sputtering gas quality

Argon (99.99% purity) was used as sputtering gas for film deposition.
The flow rate of the sputtering gas was measured by a mass-flow controller (0-200 sccm); and the Ar pressure during sputtering was measured with a capacitance vacuum meter.

4.6 Power supply

The MDX 1.5 kW MAGNETRON DRIVE, by Advanced Energy, was used to carry out the experiments.

Magnetron is connected to the power supply that is connected to National Instruments device commercially available by a cable. The NIUSB-6009 device is connected to the PC by USB connection in order to control the power supply by the program LabVIEW® USB6009 mdx-1.5K.

In Figure 27 the connections from power supply to PC are shown. The interface of the program used to perform multilayer sputtering is illustrated in Figure 28.

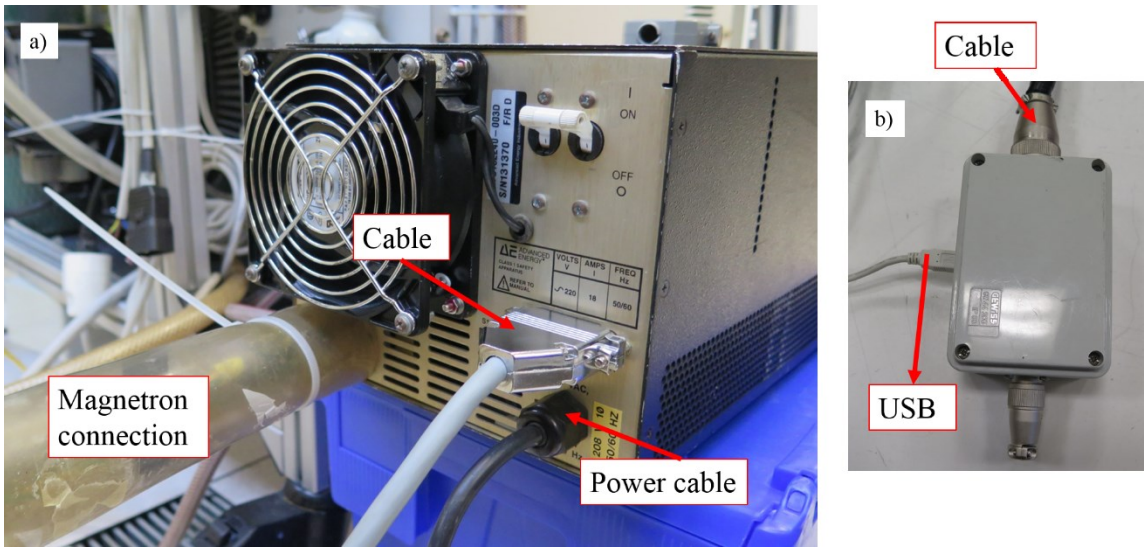

Figure 27 Power supply connections.

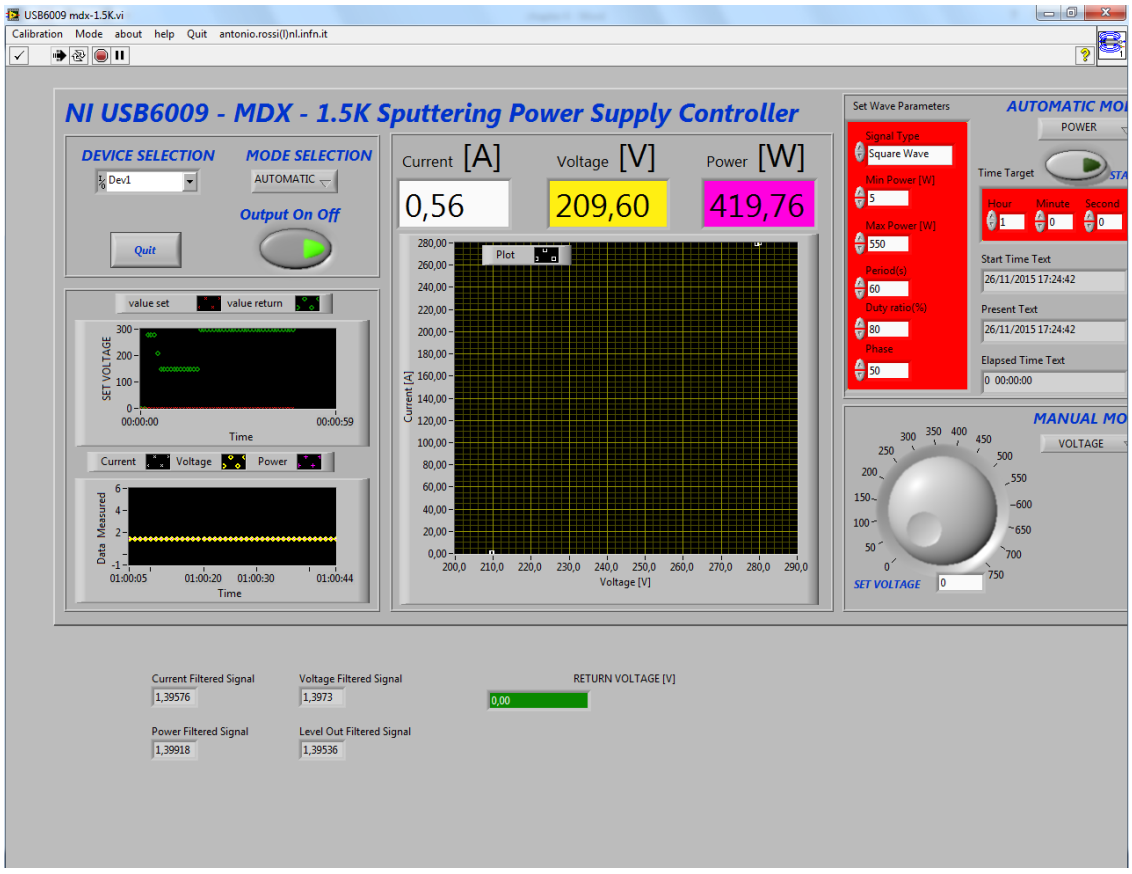

Figure 28 LabView® program interface.

4.7 Sample preparation

A base vacuum of about 1 x 10^{-6} mbar was reached before each deposition.

One critical point to take into account is the absolute cleanliness of the whole operation and the cleaning of the sputtering system. A small particle of dust left on the substrate or flakes coming from the delamination of film from the sputtering chamber, if deposited on the substrate can work as a nucleation of protrusions growing on the deposited film and amplified by the film thickness. For that reason, the substrate holder and the sample surfaces must be absolutely clean and free of dust.

Sapphire and quartz pieces were washed in ultrasound with distilled water and Rodaclean® soap for 20 minutes at 40 °C, rinsed in distilled water for 20 minutes in ultrasound and then rinsed with ethanol and dried by nitrogen gas flux.

For copper samples, NGP soap was used and the ultrasound washing step was followed by chemical etching in order to remove the oxidation (Rodasteel® soap for 20 minutes and after water in ultrasound for 20 minutes).

The magnetron was placed on the down side and the sample on the upper side, in order to avoid the dust coming from the target to compromise the cleanness of the sample surface.

4.8 Analysis Instruments

In order to analyze the deposited films in terms of thickness and microstructure, Profilometer and Scanning Electron Microscope were used.

Profilometer

Stylus profilometer Veeco – Dektat 8 was used to measure film thickness (Figure 29).
Stylus profilometer is a versatile measurement tool for studying surface topography. Its primary function is to measure film thickness by scanning step heights and trench depths. It is also useful for measuring surface planarity and thin film stress, as well as surface roughness measurements.

The stylus profilers rely on a small-diameter stylus moving along a surface by movement of the stylus. As the stylus encounters surface features, the stylus moves vertically to measure various surface features, such as deposited film and irregularities.

The stylus is mounted on an arm, coupled to a linear variable differential transformer (LVDT). During a scan, the stylus makes direct contact with the surface to obtain the data with very high precision and repeatability.

The output voltage changes from plus to minus as a function of core displacement, corresponding to the mechanical changes that occur whenever the stylus moves up and down over the features on the surface. The varying DC signal is then digitized and stored to represent the surface profile of the sample.

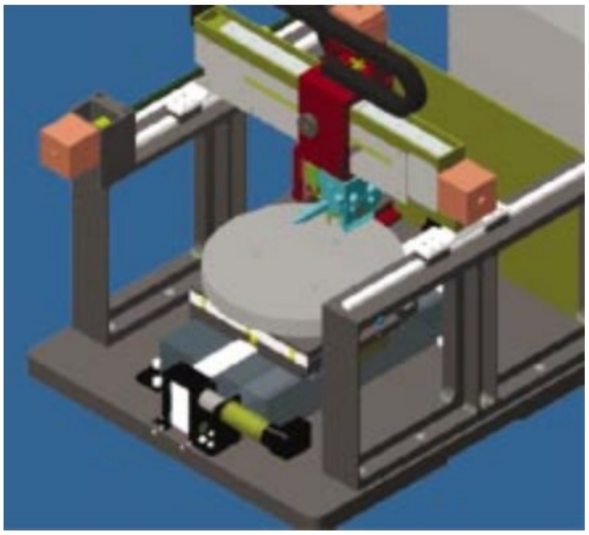

Figure 29 Scan head assembly of Dektak 8 stylus profiler with the LVDT and the scan tower, stage, scan drive, and optics.

SEM

Fei (ex Philips) Scanning Electron Microscope SEM XL-30 has been used to prove the microstructure of the deposited films.

The SEM is one of the most versatile instruments available for the examination and analysis of the microstructural characteristics of solid objects with high-resolution images (about 2 nm) compared with a resolution of about 1 μm for a conventional optical microscope. It involves scanning a fine beam of electrons over a specimen and detecting the signals, which are emitted.

Imaging in the SEM must be carried out under vacuum, as electrons cannot travel through the air. The basic components of the SEM are illustrated in Figure 30.

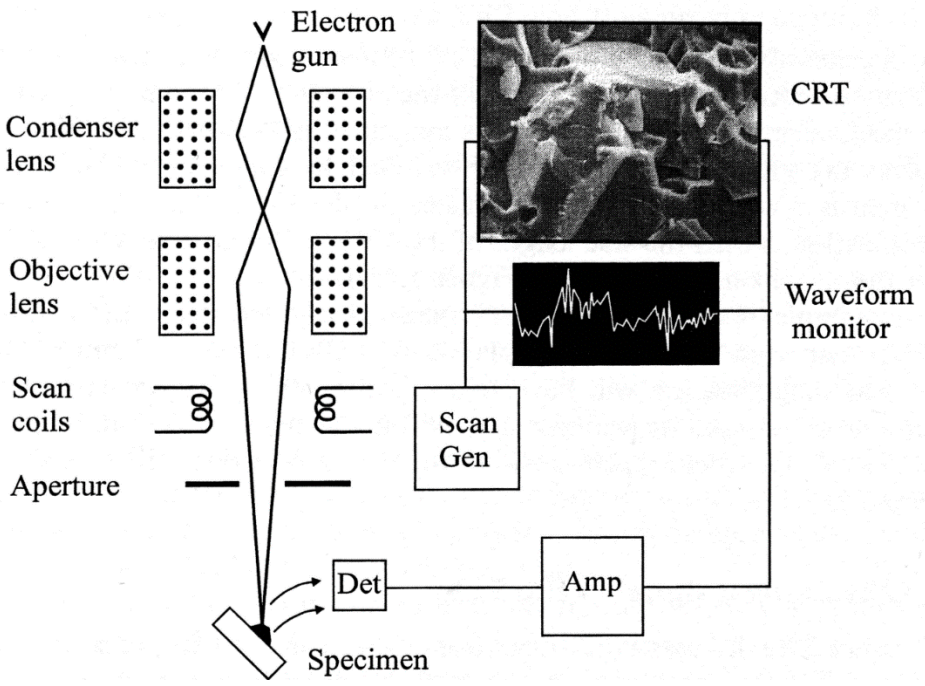

Figure 30 Basic components of SEM.

Electrons emitted by the gun are accelerated, typically by 20 kV. They pass through condenser and objective lenses, and then through a set of scan coils and an aperture. A scan is simultaneously generated on a computer monitor.

Electrons emitted by the specimen are detected and amplified; the signal is then used to produce an image.

When high-energy electrons impinge on the specimen, a number of signals are generated.

Secondary electrons originate in the specimen itself, they have an energy typically < 50 eV. They originate from within a few nm from the surface. They are therefore very sensitive to surface structure, and provide topographic information.

Backscattered electrons are high-energy electrons, which are scattered out of the specimen, losing only a small amount of energy. They originate from much deeper within the sample (a few μm below the surface), and interact much more strongly with the sample. They therefore provide compositional information, but give lower resolution images.

X-rays give information about the elemental composition of the sample.

A system of corresponding detectors allows obtaining images.

Chapter 5

Experimental results and discussion

5.1 Aim of the work

The lack of ^{99}Mo supply has made different research groups to move towards alternative routes for ^{99m}Tc production since it is the most used radioisotope in nuclear medicine.

Following preliminary feasibility studies started at LNL, in 2011, research activities have aimed to the alternative, accelerator-driven ^{99m}Tc production routes. The goal is to provide ^{99m}Tc radionuclide production, in amount that can be enough to support the diagnostic needs of Nuclear Medicine Services of the Veneto Region by using the high intensity proton cyclotron available at LNL.

The study is divided into different areas, strictly linked to each other, from the theoretical studies aimed at ^{99m}Tc direct production by proton accelerators, together with the assessment of radiochemical purity and stability of ^{99m}Tc radiopharmaceuticals and the design and development of ^{100}Mo target, and radiochemical separation/purification process.

This thesis includes the study of the development of the target production that is a crucial point. Since high proton currents involved require a target system able to remove the hitting heat power with high efficiency and be able to produce high yields of ^{99m}Tc minimizing the impurities.

The basic system consists in the target material deposited on a baking plate.
The development of the target system must take into account several requirements:

- Molybdenum film must be thick enough, dense, uniform and adherent to backing;
- The choice of a better backing material will be:
    - limited to inert material under the proton beam;
    - strictly related to the different techniques which may be exploited for the molybdenum deposition on the support plate material;

The proposed deposition technique is magnetron sputtering because of the several advantages that it can offer, even if some issues must be optimized.

This thesis is called to study the possibility to fabricate Mo target by magnetron sputtering technique optimizing sputtering parameters in order to reduce stress in thick films, and use the ceramic material as backing plate for chemical inertness.

In particular, optimal parameters were found by changing working gas pressure in order to minimize residual stress in the film and to obtain thick, adherent, dense and uniform Molybdenum films that resist under the proton beam.

Sapphire has been chosen as the backing plate because it has the highest thermal conductivity among ceramic materials and it is chemically inert during dissolution.

5.2 Possible solutions

Thick films of transition metals can be produced by a plethora of different deposition methods. Sputtering is, however, only seldom considered as a possible method for depositing thick films. The reason under that is mainly due to the fact, that sputtered films are micro-structurally stressed.

Sputtering, indeed, induces tensile or compressive stresses in the film depending on different parameters, among which the pressure of the inert gas used for igniting the discharge. Theoretically, it exists a gas pressure that signs the transition between the tensile and the compressive stress. However, this working region depends on many other parameters included the film thickness, so other aspects must be taken into account.

Therefore, the approach followed in this work consists in the stress relief due to the stress relaxation of one thousands of layered depositions of half a micron thick films. In other words the deposition of a thick film is fragmented in thousands subsequent brief depositions of thin films. Each deposition is spaced by a “relaxation time” in which the film is annealed. The idea under this method is that the stress release for half a micron film is much easier than for a hundred micron film. The hypothesis is that the deposition of a half a micron thin film will be deposited each time onto a “stress free” surface.

This procedure has been adopted for the preparation of Mo target, obtaining thick, adherent and uniform films; therefore, sputtering could be considered as a possible technique for the deposition of stress free thick films.

The choice of sapphire as backing plate is justified by the requirement of an inert material both from the point of view of inertness under the beam, and from the chemical point of view.

5.2.1 Sputtering parameter optimization

For a given a system, Argon pressure value, at which the residual stress in deposited film is minimized, could be identified. The simple way to evaluate the stress is the deposition onto a flexible substrate, e.g. KAPTON.

At the beginning, the process was developed for Nb deposition, since Nb is more available, after the method was adjusted for Molybdenum sputtering.

Argon flux optimization by using KAPTON as substrate

Niobium

The depositions were performed with the following parameters (Table 3):

Table 3 Parameters optimization (Nb on KAPTON)

Parameter optimization (Nb on KAPTON)	
Controlled in Current [A]	0,5
Target-substrate distance [cm]	6
Time	15 min
Argon flux [sccm] / $P_{working}$ [mbar]	11,5 / 1 x 10^{-2}
	10 / 8,5 x 10^{-3}

The Figure 31 shows that both deposited films present a concave curvature that means tensile stress. It is evident that the first experiment ($P_{working}$ = 1 x 10^{-2}) results in an evident tensile stress compared to the second one ($P_{working}$ = 8,5 x 10^{-3}), where the stress is almost negligible.

According to the theory, the lower the working gas pressure, the lower the tensile stress.

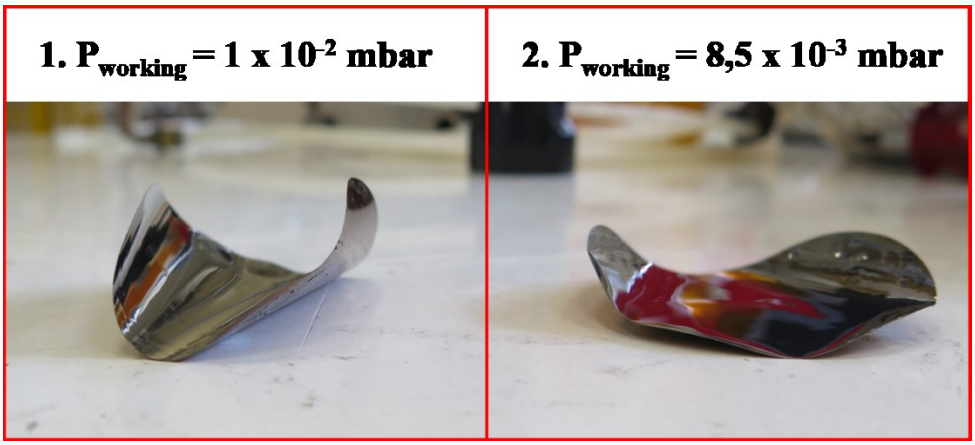

Figure 31 Resulting stress on KAPTON substrate. In experiment 1, where the $P_{working}$ was higher than that of experiment 2, the tensile stress is greater.

The best Argon flux was then found, by changing the controlled parameter from current to power (550 W). The used parameters and the results are shown in Figure 32.

Parameter optimization (Nb on KAPTON)	
Controlled in Power [W]	500
Target-substrate distance [cm]	6
Time	15 min

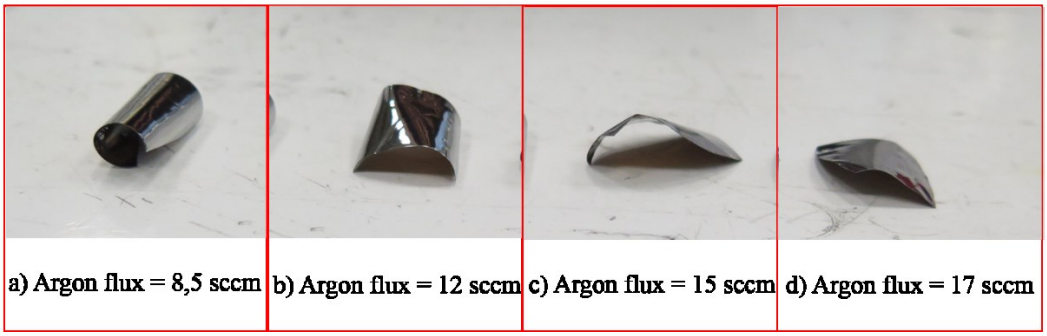

Figure 32 Influence of argon flux and so of the working pressure on film stress: higher the pressure lower the compressive stress.

In Figure 32 it can be distinctly observed the influence of argon flux and, correspondingly, the working pressure on film stress: the compressive stress is maximum in a) and it decreases from a) to d) where the stress is almost negligible.

Thus, an argon flux of 17 sccm that corresponds to a working gas pressure of 1,63 x 10^{-2} mbar, was found to be the optimal value for this system in order to avoid stress on deposited film.

Molybdenum

It was demonstrated that the parameters (Table 4) used for Niobium deposition are suitable also for natural Molybdenum, as shown in Figure 33.

Table 4 Parameter optimization (Mo on KAPTON)

Parameter optimization (Mo on KAPTON)	
Argon flux [sccm]	17
Working pressure [mbar]	1,63 x 10^{-2}
Controlled in Power [W]	550
Target-substrate distance [cm]	6 cm
Time	15 min

Figure 33 Mo film on KAPTON.

Therefore, for the deposition of thick films the sputtering process was controlled in Power (550 W) and the argon flux during deposition was 17 sccm that corresponds to a $P_{working}$ of 1,63 x 10^{-2} mbar.

5.2.2 Multilayer deposition technique: program for automated multilayer deposition

In order to reduce stress, the deposition of thick films is fragmented in thousands subsequent brief depositions of thin films (multilayer sputtering). Each deposition is spaced by a "relaxation time" in which the film is annealed. The idea under this method is that the stress release for half a micron film is much easier than for a hundred micron film. Moreover the hypothesis is that the deposition of a half a micron thin film will be deposited each time onto a "stress free" surface.

As shown in Figure 27, in chapter 4, the power supply was connected by a cable to a National Instrument device NIUSB-6009 that is interfaced with a Labview® program on the PC by USB connection.

The Labview® program allows to do thousands of depositions automatically, switching the power on and off in a programmable time with programmable intervals.

5.2.3 Temperature of the holder

The first thick film deposition, Niobium on sapphire, was performed with a water cooled sample holder but the results were not successful. The following experiments were carried out with a heated sample holder since the temperature of the holder influences the implant of atoms to the film surface and therefore the associated stress.

From the theory, an increase of substrate temperature, i.e. T/T_m ratio, is associated to the following events:

- Increase of adatom mobility;
- Increase of grain size of deposited film.

For these reasons, a heated sample holder that reaches a temperature of 500 °C was used obtaining not stressed and uniform thick films.

5.3 Thick films preparation

In this section, the experiments that led to the best recipe to obtain the optimal Mo deposition will be described and the related results will be shown.

5.3.1 Test with Nb: parameter optimization

Multilayer sputtering of Nb on thick sapphire with cooled sample holder

The first experiment involved the multilayer sputtering of Niobium on sapphire samples 1 mm thick by using the cooled sample holder. The sapphire pieces were arranged on the sample holder by using silver paint as shown in Figure 34. In Table 5, the sputtering parameters are listed.

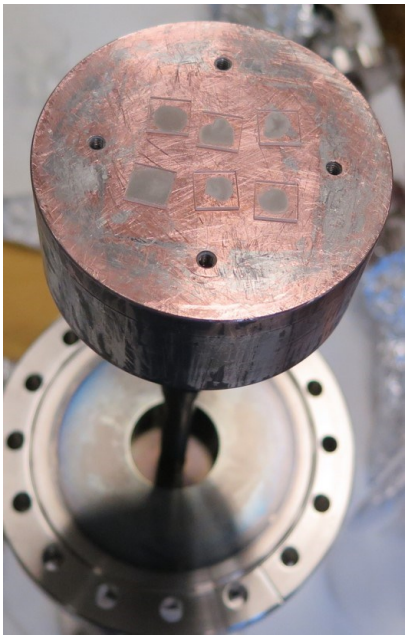

Figure 34 Six sapphire samples placed on cooled sample holder by using silver paint.

Table 5 Parameters for multilayer deposition of Nb on thick sapphire.

Multilayer sputtering of Nb on thick sapphire	
Argon flux [sccm]	9,5
Working pressure [mbar]	8×10^{-3}
Controlled in Power [W]	min 5; max 550
Temperature of the sample holder [°C]	Cooled
Target-substrate distance [cm]	6 cm
Deposition rate [µm/h]	11,5
Program for multilayer deposition	YES

This first test to produce thick-deposited films has led to unsuccessful results. In fact, as it can be seen in Figure 35, all samples are cracked and they detached from holder after different times of sputtering, from 14 h and 30 minutes, 24 h and 28 h and 30 minutes.

The possible causes are the intrinsic stress inside the films, because of the difference in thermal expansion coefficients between sapphire and Niobium and the not efficient cooling, due to a not good thermal contact. Otherwise, the quality of sapphire samples could be poor (high thickness and brittleness), or they could have interacted with plasma torch, since the II type unbalanced magnetron was used (see section 3.1).

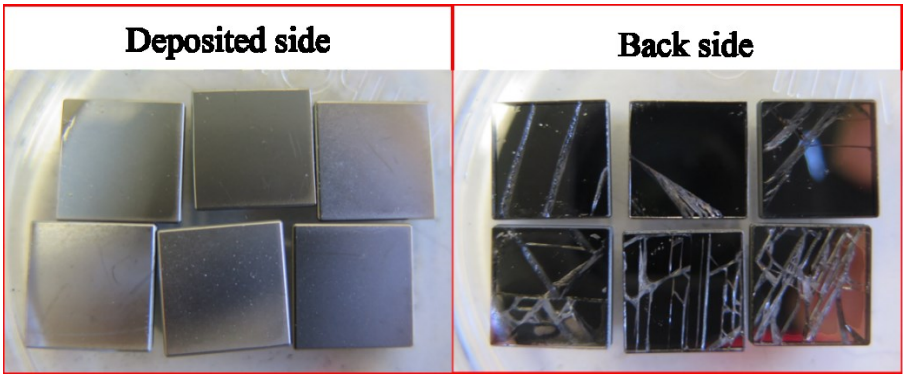

Figure 35 Results of multilayer sputtering of Nb on 1 mm thick sapphire with cooled sample holder. The deposited films seem uniform, but the sapphire is cracked.

Multilayer sputtering of Nb on thin sapphire with heated sample holder

Since the use of the cooled sample holder failed, the heated sample holder was the next choice.

Multilayer sputtering of Nb on thin (100 μm) pieces of sapphire was tested by using the heated sample holder at 500 °C.

The samples were placed on the holder by mean of screws as illustrated in Figure 36, and sputtering was performed with the parameters summarized in Table 6.

Figure 36 Arrangement of thin sapphire samples with screws.

Table 6 Parameters for multilayer deposition of Nb on thin sapphire.

Multilayer sputtering of Nb on thin sapphire	
Argon flux [sccm]	9,5
Working pressure [mbar]	8×10^{-3}
Controlled in Power [W]	min 5; max 550
Temperature of the sample holder [°C]	450
Target-substrate distance [cm]	7 cm
Deposition rate [μm/h]	12
Program for multilayer deposition	YES

The parameters seems to be not suitable for this kind of deposition because in the resulting films compressive stress is evident as illustrate in Figure 37. Furthermore, the sapphire is cracked. It could be deduced that the arrangement of the samples with the screws is not suitable for a very thin sapphire because it is very brittle; in fact, it is possible that during the increasing of the temperature, the screws, with higher thermal expansion coefficient in comparison with sapphire, have compressed the samples, cracking them.

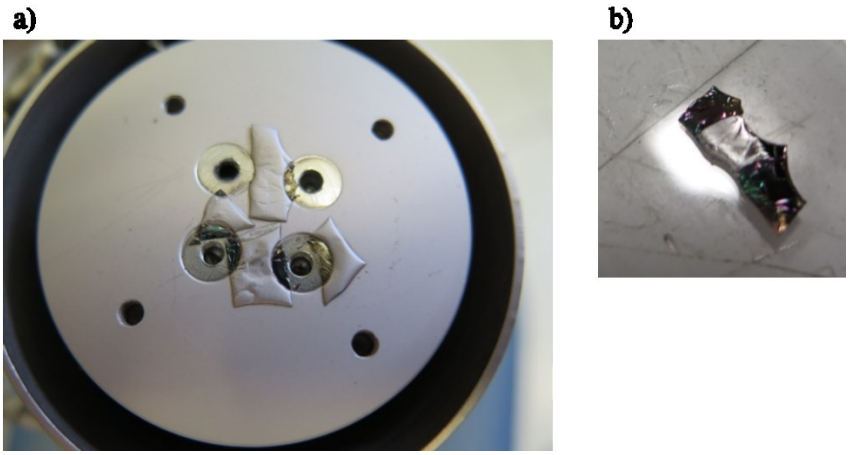

Figure 37 Results of multilayer sputtering of Nb on thin sapphire with heated sample holder. The deposited films are subjected to compressive stress (a), and the sapphire is cracked (b).

Multilayer sputtering of Nb on Quartz with heated sample holder

In the following experiment, the gas pressure was increased in order to decrease the compressive stress. Nb was multilayer sputtered on quartz samples with the parameters listed in Table 7.

The samples were arranged in the same way of the previous experiment (with screws) as it is shown in Figure 38 a).

The results illustrated in Figure 38 b), c) and d) clearly demonstrate that the parameters are not suitable for quartz samples.

Table 7 Parameters for multilayer deposition of Nb on quartz.

Multilayer sputtering of Nb on quartz	
Argon flux [sccm]	17
Working pressure [mbar]	$1{,}63 \times 10^{-2}$
Controlled in Power [W]	min 5; max 550
Temperature of the sample holder [°C]	450
Target-substrate distance [cm]	6 cm
Deposition rate [µm/h]	10,26
Program for multilayer deposition	YES

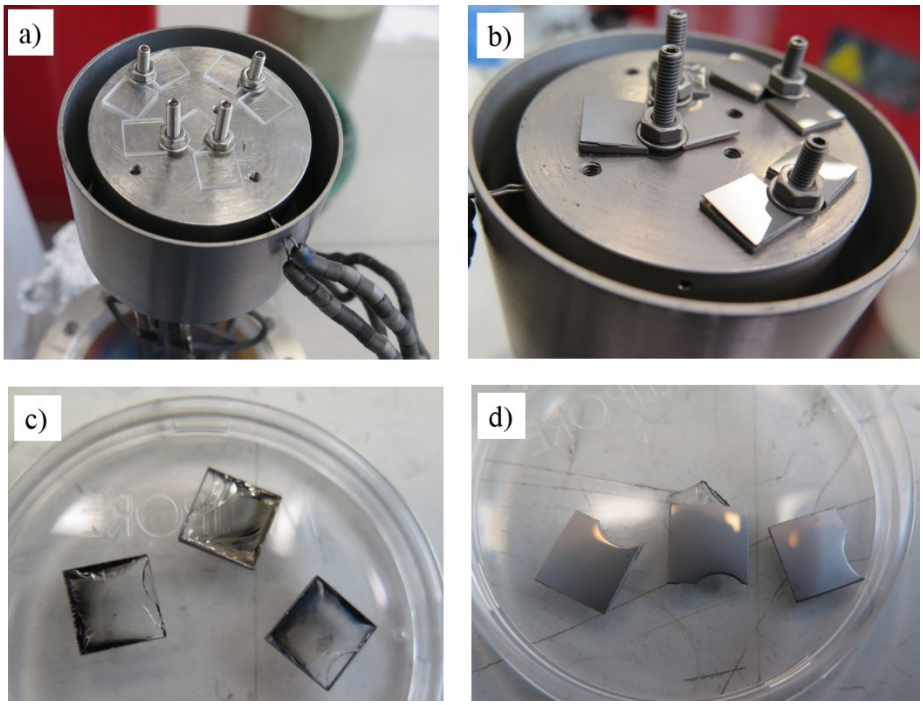

Figure 38 Multilayer sputtering of Nb on quartz with heated sample holder. a) Arrangement of the sample with screws; b) Results after sputtering; c) Cracked quartz; d) Deposited films.

In fact, Nb films have not adhered to the quartz, as can be seen in Figure 38 b). The deposited films are detached from the quartz substrates probably because of the different thermal expansion coefficient between quartz pieces and Nb films (0,6 x 10^{-6} / °C and 7,31 x 10^{-6} / °C respectively); quartz is also cracked (Figure 38 c)).

The thickness of the films results 130,3 ± 3,5 µm and they seem not stressed.

In the following experiments, the sapphire pieces are tested with the same parameters since the sapphire material has a thermal expansion coefficient quite similar to the Niobium one.

Multilayer sputtering of Nb on Sapphire with heated sample holder

Thin and thick sapphires (Figure 39 a)) were sputtered with Nb by using the parameters listed in Table 8.

Thick Nb films on thick sapphire samples showed the following results:

- ✓ Not stressed
- ✓ Adherent to the substrate
- ✓ The substrates are not cracked,

as shown in Figure 39 b), and after 10 h of sputtering, the thickness of the film about 84 ± 3,65 µm was obtained.

Table 8 Parameters for multilayer deposition of Nb on thin and thick sapphire.

Multilayer sputtering of Nb on sapphire	
Argon flux [sccm]	17
Working pressure [mbar]	1,63 x 10^{-2}
Controlled in Power [W]	min 5; max 550
Temperature of the sample holder [°C]	500
Target-substrate distance [cm]	6 cm
Deposition rate [µm/h]	8,4
Program for multilayer deposition	YES

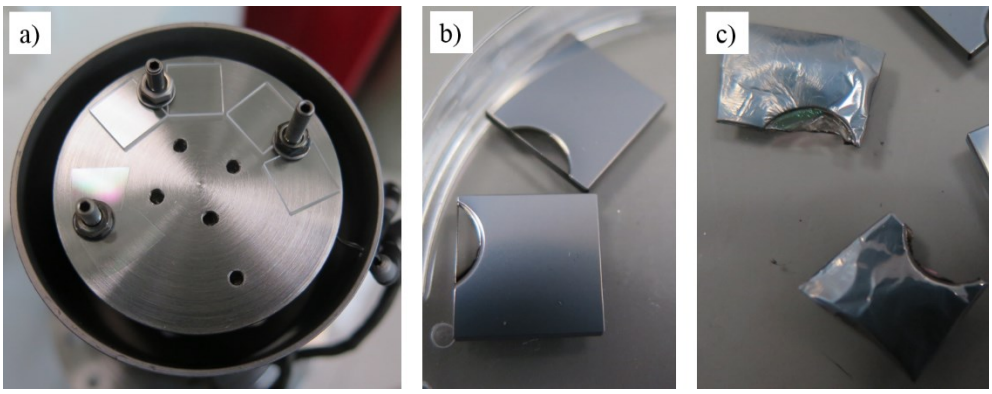

Figure 39 Multilayer sputtering of Nb on thick and thin sapphire with heated sample holder. a) Arrangement of the sample with screws; b) Coated thick sapphire; c) Coated thin sapphire.

Instead, the resulting films on thin sapphires (Figure 39 c)) were stressed, even if the compressive stress seems to be lower than that obtained in the previous experiment (Figure 37 (thin sapphire)), surely because a higher working pressure was used (1,63 x 10^{-2} mbar).

In conclusion, the parameters used in the last experiment gave successful results in terms of uniformity, adhesion and stress free of Nb film. Therefore, we moved to natural Molybdenum target in order to understand if the same parameters were suitable.

5.3.2 Mo Sputtering: Parameter Optimization

Once verified that the parameters optimized for Nb film gave good results on sapphire (Figure 39), 5 µm thick films of Mo on sapphire and quartz were produced by using the program that automates the multilayer deposition.

In addition a silicon wafer was used as a substrate, in order to obtain a cross section of the film for the microstructure analysis with SEM.

From a qualitative evaluation (Figure 40), the coating on sapphires is uniform and not stressed in comparison to the quartz samples.

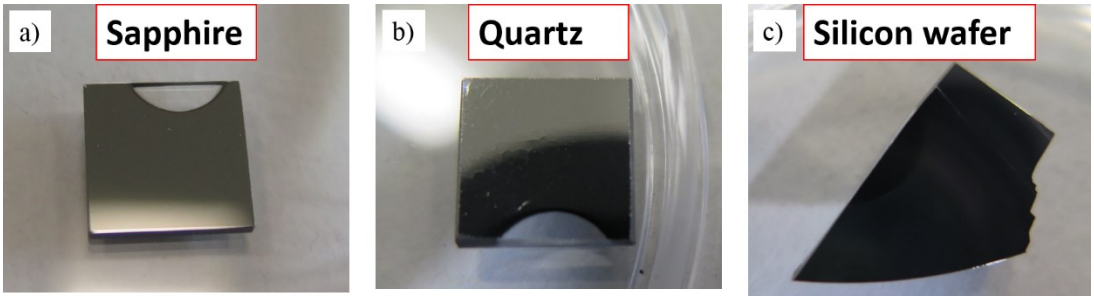

Figure 40 5 µm Mo deposition on sapphire, quartz and silicon wafer.

Through the analysis with SEM the stress and the cracks of the film on quartz samples are evident (Figure 41 b)). On the contrary, the deposition is uniform and no cracks are observed on sapphire (Figure 41 a)).

These results confirm that the difference of about one order of magnitude in thermal expansion coefficient, between quartz and Mo, leads to a stress that causes cracking in the films.

Instead, the deposition on sapphire results “stress free” in fact the thermal expansion coefficient of sapphire and Mo is quite similar, 6 x 10^{-6} / K and 4,8 x 10^{-6} / K respectively.

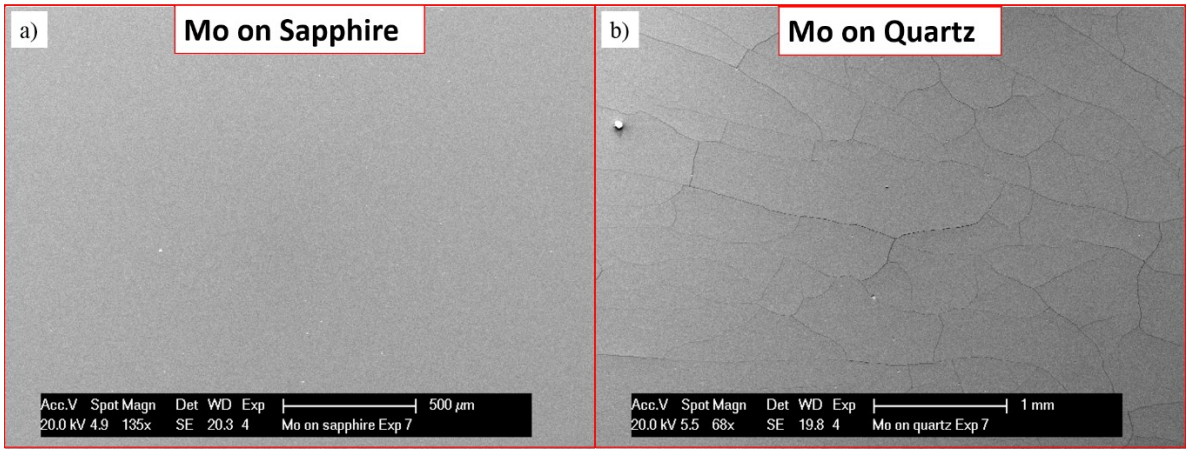

Figure 41 SEM images of deposited Mo on sapphire (a) and quartz (b).

Observing the SEM image of the cross section obtained from silicon wafer sample, in Figure 42 a), it can be noted that the microstructure of the film is columnar and the grain size is of the order of about hundreds nm (Figure 42 b)). The temperature of the holder provides denser microstructure thanks to renucleation. In addition, the temperature of the holder, reached slowly, allows not to increase the stress, due to the difference of thermal expansion coefficient of film and substrate.

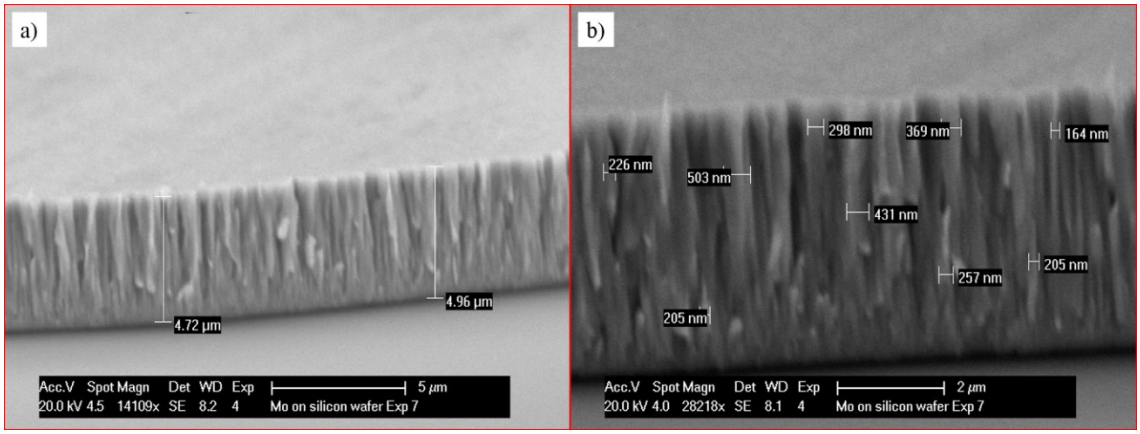

Figure 42 Cross section SEM images of Mo deposition. a) Mo film (~5 µm) presents a columnar microstructure; b) the grain size is of order of about hundreds nm.

Since the parameters used in this experiment gave good results in terms of film density and uniformity on silicon and sapphire substrates, thicker films have been prepared on sapphire and copper coins placed on the sample holder with screws, as illustrated in Figure 43.

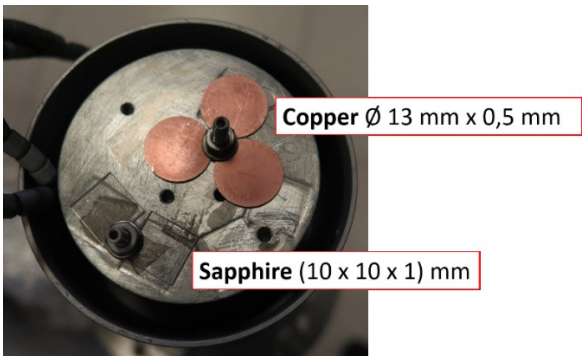

Figure 43 Two Sapphires and Three Copper coins arranged on the sample holder with screws.

Therefore, with the best parameters found (Table 9), after 10 hours of sputtering, films of about 110 µm ± 2 µm thickness have been obtained.

Despite this thickness, the films were uniform and not stressed, as illustrated in Figure 44.

Table 9 Optimal parameters for Mo thick film preparation.

Multilayer sputtering of Mo on sapphire and copper	
Argon flux [sccm]	17
Working pressure [mbar]	1,63 x 10^{-2}
Controlled in Power [W]	min 5; max 550
Temperature of the sample holder [°C]	500 (~ 4 °C/min)
Target-substrate distance [cm]	6 cm
Deposition rate [µm/h]	11
Program for multilayer deposition	YES

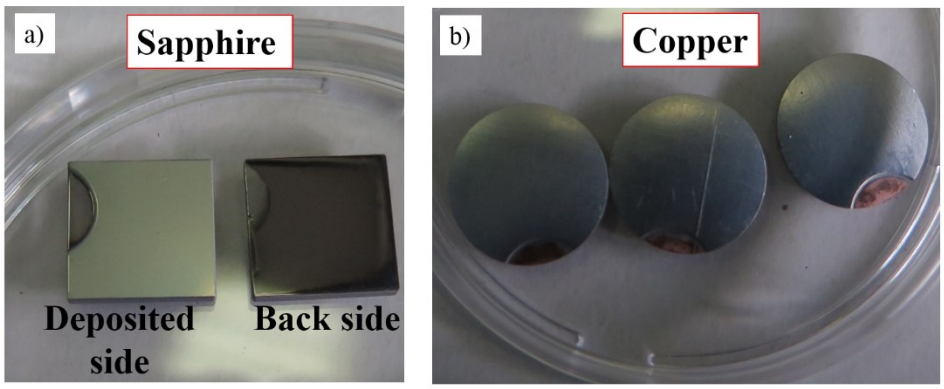

Figure 44 Thick molybdenum films on sapphire (a) and copper coins (b).

Furthermore, the back side of the sapphire piece showed its integrity, in fact, the thermal expansion coefficients of sapphire and Molybdenum are quite similar (6 x 10^{-6} / K and 4,8 x 10^{-6} / K respectively).

A thickness of about 100 μm should be the desirable thickness for the Mo target for the production of ^{99m}Tc by 16 MeV cyclotron.

5.3.3 Sapphire and copper coins

Mo thick film were also prepared on sapphire pieces with diameters of 13 mm and thickness of 0,5 mm.

A copper mask was used to fix the samples on the sample-holder as shown in Figure 45 in order to provide

- ✓ **Good thermal conductivity** between the samples and the holder in order to heat the samples at 500 °C during sputtering
- ✓ **Safe arrangement** of sapphire pieces
- ✓ Possibility to sputter **six samples** simultaneously.

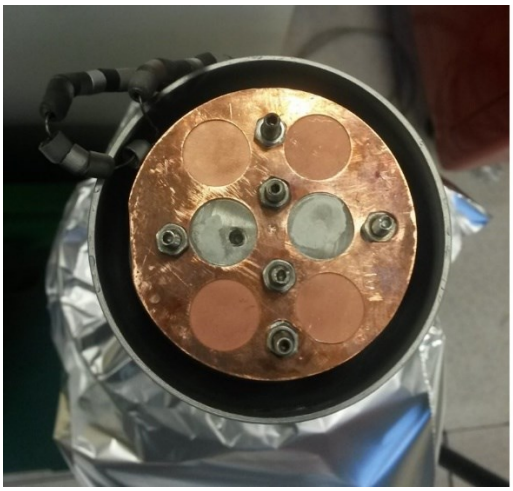

Figure 45 4 copper coins and 2 sapphire coins fixed with a copper mask on the sample holder.

The sapphire pieces were fixed with silver paint, too.

The thickness obtained, after 6 hours of sputtering with 500 W power and argon flux variable from 27 to 17, was about 90 µm. The resulted Mo films (Figure 46) were not stressed and the sapphire samples were not cracked as it can be seen in the picture.

In this experiment, different parameters were used because Mo target was too thick for the magnetron configuration used or because of the presence of very thick oxidized layer on the Mo target.

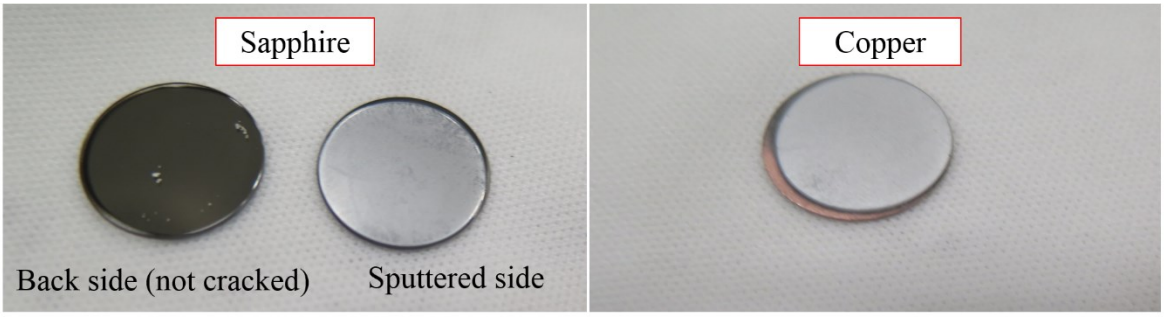

Figure 46 90 µm on natural Mo sputtered on sapphire and copper coins.

These samples were tested in the cyclotron in Sant'Orsola hospital in Bologna in order to evaluate the behavior of the sputtered natural Mo thick film, under the beam with different irradiation currents.

5.4 Cyclotron irradiation

For the irradiation test with the cyclotron in Sant'Orsola Hospital in Bologna, a target holder was fabricated by the mechanical workshop in LNL.

The copper 4-pin target holder, shown in Figure 47, allows placing the 13 mm diameter coins and cooling down the frontal side of the target, with Helium jet, during the irradiation.

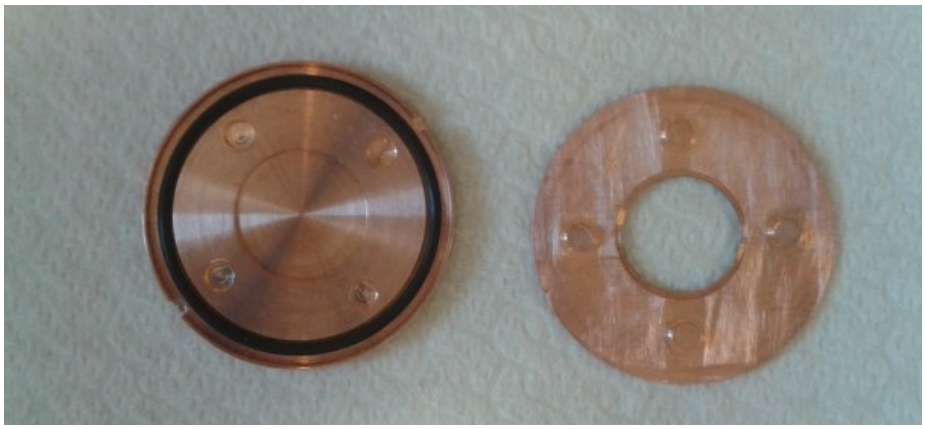

Figure 47 Target holder for cyclotron test.

This target holder is manually placed inside the cyclotron as shown in Figure 48 b) and it is automatically unloaded after irradiation. During irradiation, the proton beam hits Havar® foil, enters the chamber, hits Mo target that is cooling down by Helium jet; on the back side of the target there is a piston that employs a force to keep the target pressed; the piston also provides, a water cooling system (Figure 48 a)). In Figure 48 b) the cyclotron with the automatic unloading of the target is illustrated.

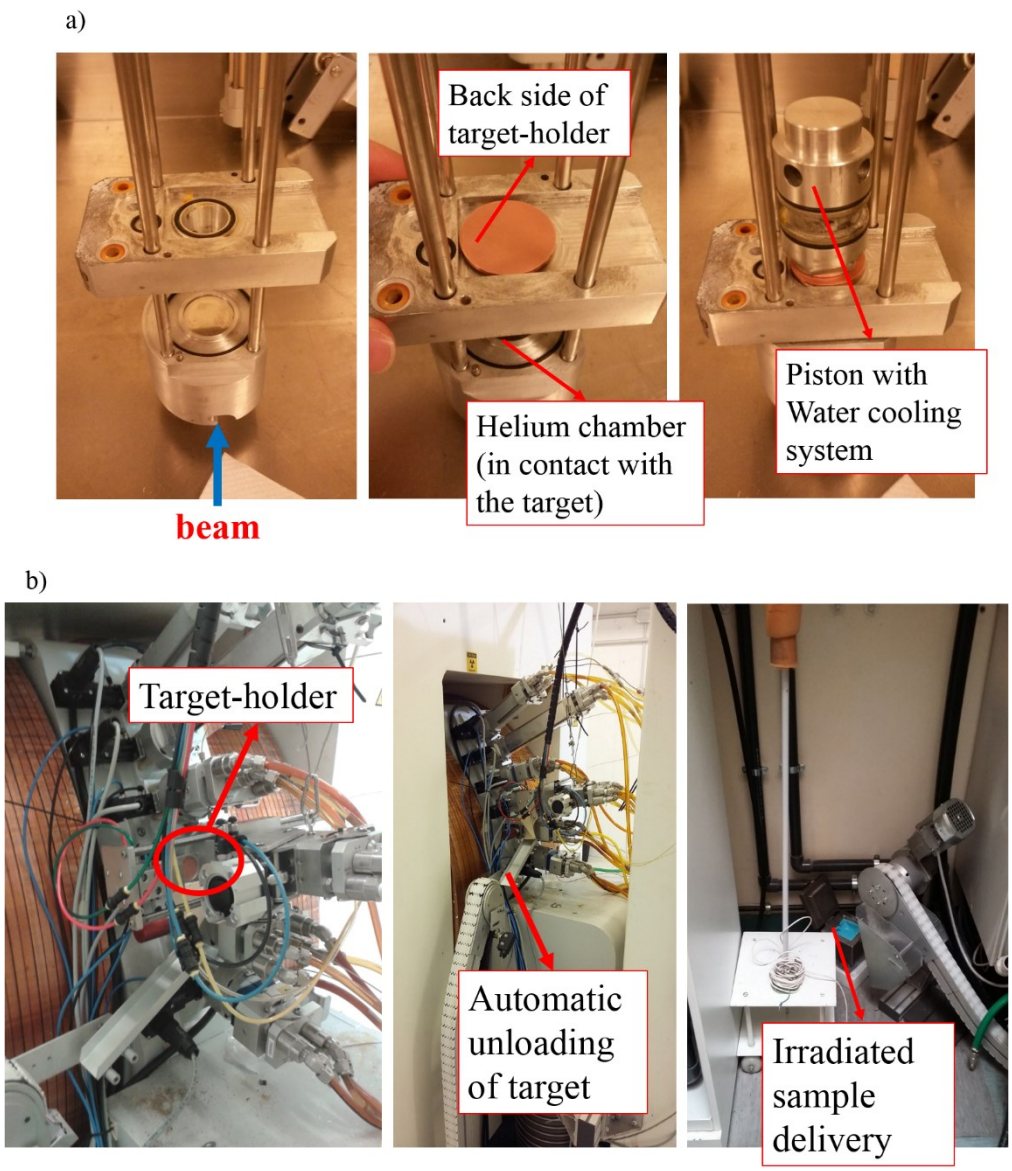

Figure 48 a) target holder inside the cyclotron; b) cyclotron.

90 µm of Natural Mo sputtered on sapphire coin was placed inside the target holder with 2 copper foils in order to provide a better thermal contact (Figure 49).

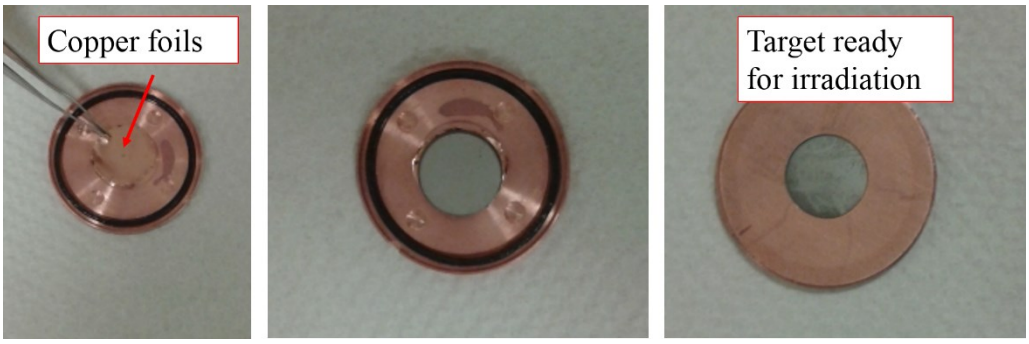

Figure 49 Sapphire coin inside the target holder ready for irradiation.

The irradiation tests were carried out for one minute, at current:

- 10 µA;
- 20 µA;
- 30 µA;
- 50 µA.

After 30 minutes of each irradiation, the sample was unloaded and controlled visually.

In Figure 50 the target after each irradiation is shown: 90 µm of Mo sputtered on 0,5 mm sapphire resisted under the beam current of 10 µA (Figure 50 a)) and 20 µA (Figure 50 b)) and the sapphire was not cracked. Instead, for a current of 30 µA (Figure 50 c)) the sapphire backing was cracked but the Mo film kept the pieces together, proving a good performance of sputtered Mo film under the beam in terms of good adhesion, no delamination and no clear oxidation. On the contrary, the target was cracked into 2 pieces under the proton beam at 50 µA (Figure 50 d)).

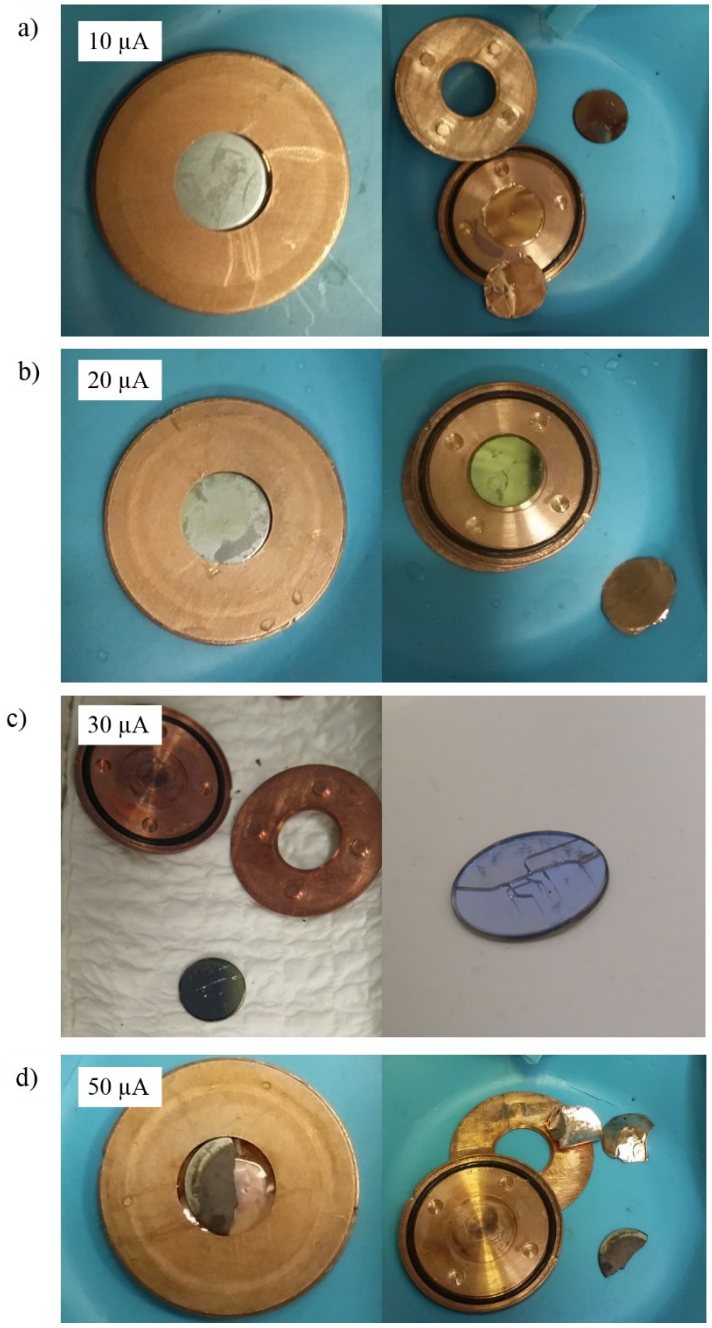

Figure 50 Results after irradiations test: a) 10 µA for 1 minute; b) 20 µA for 1 minute; c) 30 µA for 1 minute; d) 50 µA for 1 minute.

5.5 Dissolution test and γ-spectroscopy analysis

In order to prove the chemical inertness of sapphire backing, dissolution tests followed by γ-spectroscopy analysis were performed thanks to the Research Laboratory of Sant'Orsola Hospital Medical Physic Department (Bologna).

At first, a non-irradiated sample (110 µm of Mo onto 1 mm thick sapphire) was dissolved in 1,5 ml of H_2O_2 30% at 70 °C. The dissolution continued until bubbles came out

from the coated surface. After 30 minutes, the reaction ended because the surface was fully oxidized. In order to restart the reaction, saturated H_2O_2 was removed and 1,5 ml of fresh H_2O_2 30% was added. In this way, the reaction restarted until the complete dissolution of Mo film (Figure 51).

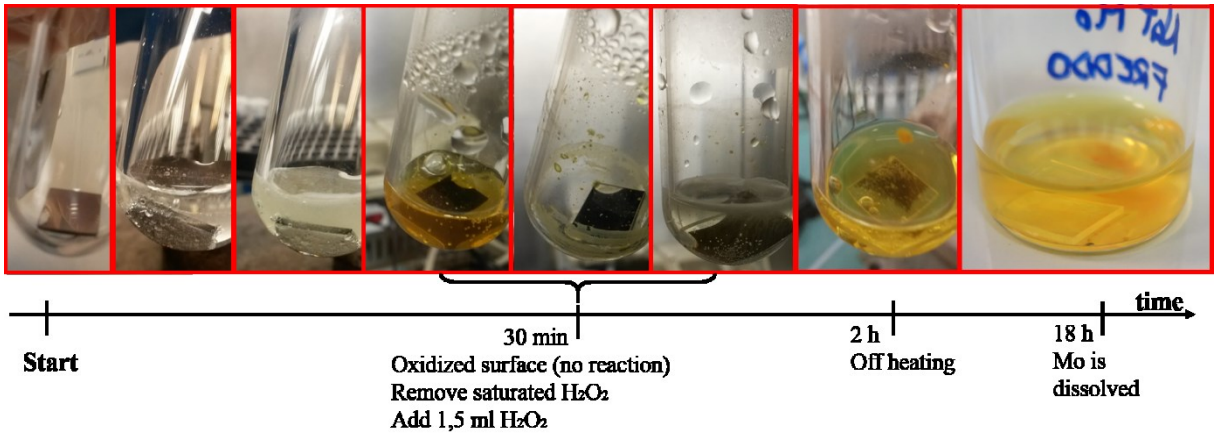

Figure 51 Dissolution test of not-irradiated sample.

This experiment has proved that thick Mo film dissolves in H_2O_2 with heating after several hours.

A piece of irradiated target (50 μA, Figure 50) was used for a dissolution test, described in Figure 52, followed by γ-spectroscopy analysis in order to asses if some impurities coming from irradiated sapphire were present in the solution.

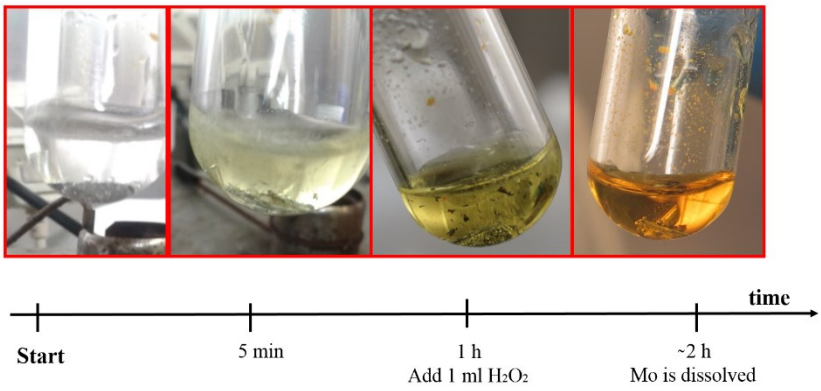

Figure 52 Dissolution test of irradiated sample.

10 µl of this solution were placed in the γ-spectrometer for 10 hours (live time). The range of the γ-rays energy was 80 – 4096 keV.

According to the software the peaks belonging to ^{92m}Nb, ^{94}Tc, ^{95}Tc, ^{95m}Tc, ^{96}Tc, ^{99}Mo, ^{99m}Tc were identified (Table 10). All these radionuclides are the irradiation products of natural Molybdenum. Indeed, ^{92m}Nb comes from the reaction ^{95}Mo(p,α); all the other radionuclides are produced by a set of (p,xn) reactions starting from the natural molybdenum isotopes: ^{92}Mo, ^{94}Mo, ^{95}Mo, ^{96}Mo, ^{97}Mo, ^{98}Mo, ^{100}Mo [14], [32].

Therefore, any contaminant is present in the solution, proving the chemical inertness of sapphire.

Table 10 γ-spectroscopy analysis report.

Tipo di Campione: Campione Mo naturale
Libreria di Nuclidi usata: C:\GENIE2K\CAMFILES\Mo_decay_corr_no96Tc

IDENTIFIED NUCLIDES

Nuclide Name	Id Confidence	Energy (keV)	Yield (%)	Activity (Bq /.)	Activity Uncertainty
NB-92m	0.998	912.73	1.78		
		934.46*	99.00	2.841E+001	5.460E+000
TC-94	0.902	449.20	3.30		
		532.10	2.35		
		702.62*	99.60	3.680E+003	3.097E+002
		742.30	1.21		
		849.74*	95.70	1.511E+005	7.862E+003
		871.09*	100.00	4.568E+003	2.654E+002
		916.10	7.60		
		1592.10*	2.25	3.855E+004	5.607E+003
TC-95	0.992	765.79*	93.82	1.944E+004	8.073E+002
		947.67*	1.95	1.816E+004	1.224E+003
		1073.71*	3.74	2.017E+004	1.095E+003
TC-95m	0.999	204.12*	63.25	2.887E+002	1.729E+001
		582.08*	29.96	2.620E+002	5.110E+001
		616.49	1.28		
		786.20	8.66		
		820.62*	4.71	2.798E+002	1.011E+002
		835.15*	26.63	2.365E+002	1.991E+001
		1039.26	2.78		
TC-96	0.985	314.34*	2.43	1.149E+004	1.503E+003
		316.27	1.40		
		778.22*	100.00	6.895E+003	2.845E+002
		812.58*	82.00	6.923E+003	5.295E+002
		849.93*	98.00	7.121E+003	4.913E+002
		1091.35*	1.10	7.174E+003	8.664E+002
		1126.96*	15.20	6.871E+003	7.324E+002
MO-99	0.981	40.58	1.05		
		140.51*	89.43	5.822E+002	2.816E+001
		181.06*	5.99	2.552E+002	6.997E+001
		366.42	1.19		
		739.50*	12.13	2.212E+002	6.796E+001
		777.92*	4.26	1.761E+005	7.909E+003
TC-99m	0.936	140.51*	89.00	3.968E+003	5.495E+002

* = Energy line found in the spectrum.

Conclusion

The direct production on ^{100}Mo enriched targets is the most promising production way of large quantities of ^{99m}Tc using high current cyclotrons (500 μA, at energies Ep=~20 MeV). The estimated daily quantities, in terms of activity, for medical procedures is 6-7 Ci, enough for regional needs of nuclear medicine services (e.g. the Veneto Region).

After theoretical studies about the energy needed to produce large amounts of ^{99m}Tc by proton-accelerator route, the development of a solid target represent a critical point.

In this thesis, a development of an innovative target system has been proposed: it consists in a Mo film deposited onto an appropriate backing plate. Specifically, magnetron sputtering technique was used to produce Mo films and sapphire was proposed as the material for the backing plate.

The best sputtering parameters were found after several experiments. The high temperature of the sample holder (500 °C) and the suitable working pressure, optimized for this system (1,63 x 10^{-2} mbar), have given the best Mo films in terms of adhesion, density and stress-free despite the thickness (~ 100 μm). Indeed, the fact that high thickness Mo films were deposited onto brittle substrates, as sapphires, which is unusual for sputtering, and without damaging the substrate, is proving the efficiency of the developed sputtering technique to provide stress-free films.

During the irradiation tests under the cyclotron accelerated proton beam, 90 μm of natural Mo sputtered onto sapphire coins showed high adherence, no-oxidation and no-delamination.

The system 90 μm of natural Mo on 0,5 mm sapphire has resisted up to 30 μA of proton beam with the use of a custom-made target holder system with the cyclotron in Sant'Orsola Hospital in Bologna.

Sapphire has revealed to be a suitable backing material for the target system; in fact, γ-spectroscopy has proved the absence of radioisotope contaminations in the solution of dissolved Mo.

Future works

Surely, a current of 30 μA and 1 minute of irradiation are quite low for the production of large amount of ^{99m}Tc, so the system should be improved in order to be able to resist at higher powers.

Synthetic diamonds will be taken into account as backing plate material, since they have higher thermal conductivity than sapphires.

When the target system will be improved to use higher irradiation currents, the next step will be to move toward deposition of Mo targets enriched with isotope ^{100}Mo.

^{100}Mo material is provided in powder form, so it is necessary to develop a method to fabricate a dense target, suitable for sputtering process, starting from powders.

However, it must be kept into account that ^{100}Mo is an extremely expensive isotope of Mo, so the preparation of a thick target at a reasonable cost already represents a technological challenge.

Magnetron sputtering is a very low target utilization technique; therefore, it is necessary to develop a suitable strategy for the deposition of a very small amount of material to reduce the loss of the very expensive ^{100}Mo target.

II type unbalanced magnetron sputtering exploits only 20-30% of the total target material. In Figure 53 a standard 2 inches metallic target before and after sputtering until its complete erosion is shown.

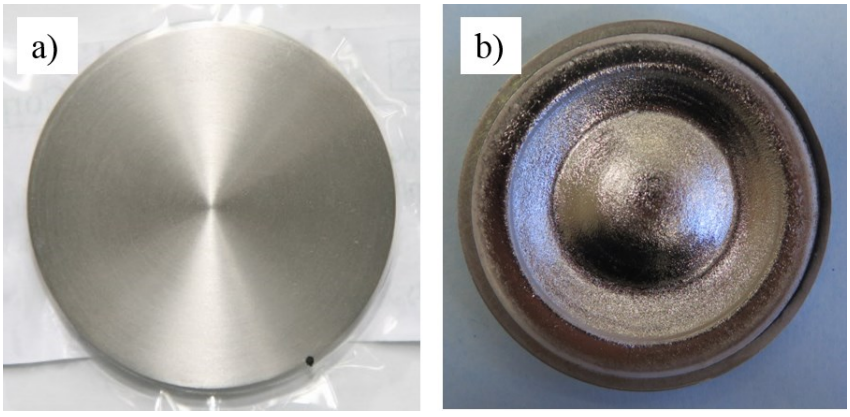

Figure 53 Standard 2 inches target before (a) and after (b) magnetron sputtering.

Therefore, a high amount of target is lost.

In order to reduce this loss, some proposals have been planned:

- to continue to use 2 inches target following the idea to erode a natural Mo target, enlarge the eroded trace, and full the vacation by pressing and sintering the ^{100}Mo powder. In this way, the expensive ^{100}Mo powder enriched should be preserved, since about 20 g of target are need, rather than 130 g, for each deposition (six targets);
- the erosion profile depends on the plasma confinement due to the magnets displacement, so that, modifying it, a more uniform erosion of the target could be achieved, taking into account that the magnetic field lines must born and die on the target and the lines $\vec{E}\ x\ \vec{B}$ must be annularly closed;
- alternative solution could be to decrease the size of magnetron and the target, respectively.

Furthermore, the problem of the material loss, due to the large cone of sputtering, can be eventually solved by the use of suitable shutters, from which ^{100}Mo can be recovered, and by designing a non-planar source, especially suited for a directional deposition.

For high production of ^{99m}Tc, the high power involved requires a suitable design of target holder, able to release heat quickly; the development of this target holder and of a suitable cooling system is currently under investigation at LNL.

List of figures

List of tables

Bibliography

[1] J. Vucina, N. Nikolic, and D. Petrovic, “Technetium-99m in production and use,” *Nucl. Technol. Radiat. Prot.*, vol. 24, no. 1, pp. 68–73, 2009.

[2] P. Schaffer, F. Bénard, A. Bernstein, K. Buckley, A. Celler, N. Cockburn, J. Corsaut, M. Dodd, C. Economou, T. Eriksson, and others, “Direct Production of 99mTc via 100Mo (p, 2n) on Small Medical Cyclotrons.”

[3] J. Esposito, G. Vecchi, G. Pupillo, A. Taibi, L. Uccelli, A. Boschi, and M. Gambaccini, “Evaluation of and Productions Based on a High-Performance Cyclotron,” *Sci. Technol. Nucl. Install.*, vol. 2013, pp. 1–14, 2013.

[4] V. N. Richards, E. Mebrahtu, and S. E. Lapi, “Cyclotron Production of 99mTc using 100Mo2C targets,” *Nucl. Med. Biol.*, vol. 40, no. 7, pp. 939–945, Oct. 2013.

[5] B. Guérin, S. Tremblay, S. Rodrigue, J. A. Rousseau, V. Dumulon-Perreault, R. Lecomte, J. E. van Lier, A. Zyuzin, and E. J. van Lier, “Cyclotron production of 99mTc: an approach to the medical isotope crisis,” *J. Nucl. Med.*, vol. 51, no. 4, p. 13N–16N, 2010.

[6] “TR RCM2 Final Report Draft oct 22nd clean copy.pdf.” .

[7] J. Beaver and H. Hupf, “Production of 99mTc on a medical cyclotron: a feasibility study,” *J. Nucl. Med.*, vol. 12, no. 11, pp. 739–741, 1971.

[8] L. Besra and M. Liu, “A review on fundamentals and applications of electrophoretic deposition (EPD),” *Prog. Mater. Sci.*, vol. 52, no. 1, pp. 1–61, Jan. 2007.

[9] V. Hanemaayer, F. Benard, K. R. Buckley, J. Klug, M. Kovacs, C. Leon, T. J. Ruth, P. Schaffer, and S. K. Zeisler, “Solid targets for 99mTc production on medical cyclotrons,” *J. Radioanal. Nucl. Chem.*, vol. 299, no. 2, pp. 1007–1011, Feb. 2014.

[10] B. A. Thomas, J. S. Wilson, and K. Gagnon, “Solid 100Mo target preparation using cold rolling and diffusion bonding.”

[11] “34 Zeisler WTTC15 Proceedings kw.pdf.” .

[12] K. Gagnon, J. S. Wilson, C. M. B. Holt, D. N. Abrams, A. J. B. McEwan, D. Mitlin, and S. A. McQuarrie, “Cyclotron production of 99mTc: Recycling of enriched 100Mo metal targets,” *Appl. Radiat. Isot.*, vol. 70, no. 8, pp. 1685–1690, Aug. 2012.

[13] S. Swann, “Magnetron sputtering,” *Phys. Technol.*, vol. 19, no. 2, p. 67, 1988.

[14] H. Targholizadeh, G. Raisali, A. R. Jalilian, N. Rostampour, M. Ensaf, and M. K. Dehghan, “Cyclotron production of technetium radionuclides using a natural metallic molybdenum thick target and consequent preparation of [Tc]-BRIDA as a radio-labelled kit sample,” *Nukleonika*, vol. 55, no. 1, pp. 113–118, 2010.

[15] P. J. Kelly and R. D. Arnell, “Magnetron sputtering: a review of recent developments and applications,” *Vacuum*, vol. 56, no. 3, pp. 159–172, 2000.

[16] F. Spaepen, “Interfaces and stresses in thin films,” *Acta Mater.*, vol. 48, no. 1, pp. 31–42, 2000.

[17] D. M. Mattox, “Atomistic film growth and resulting film properties: residual film stress,” *Vac. Technol. Coat.*, pp. 22–23, 2001.

[18] E. Bemporad, M. Sebastiani, F. Casadei, and F. Carassiti, “Modelling, production and characterisation of duplex coatings (HVOF and PVD) on Ti–6Al–4V substrate for specific mechanical applications,” *Surf. Coat. Technol.*, vol. 201, no. 18, pp. 7652–7662, Jun. 2007.

[19] A. J. Detor, A. M. Hodge, E. Chason, Y. Wang, H. Xu, M. Conyers, A. Nikroo, and A. Hamza, “Stress and microstructure evolution in thick sputtered films,” *Acta Mater.*, vol. 57, no. 7, pp. 2055–2065, Apr. 2009.

[20] T. Karabacak, J. J. Senkevich, G.-C. Wang, and T.-M. Lu, “Stress reduction in sputter deposited films using nanostructured compliant layers by high working-gas pressures,” *J. Vac. Sci. Technol. Vac. Surf. Films*, vol. 23, no. 4, p. 986, 2005.

[21] T. J. Vink, M. A. J. Somers, J. L. C. Daams, and A. G. Dirks, “Stress, strain, and microstructure of sputter-deposited Mo thin films,” *J. Appl. Phys.*, vol. 70, no. 8, pp. 4301–4308, 1991.
[22] “Stress_in_Thin_Films.pdf.” .
[23] P. M. Martin, Ed., *Handbook of deposition technologies for films and coatings: science, applications and technology*, 3. ed. Amsterdam: Elsevier, 2010.
[24] K. O’Donnell, J. Kostetsky, and R. Post, “Stress control in NiV, Cr and TiW thin films used in UBM and backside metallization,” in *Flip Chip Technology Conference (Austin, Texas, 2002)*, 2002.
[25] A. J. Detor, A. M. Hodge, E. Chason, Y. Wang, H. Xu, M. Conyers, A. Nikroo, and A. Hamza, “Stress and microstructure evolution in thick sputtered films,” *Acta Mater.*, vol. 57, no. 7, pp. 2055–2065, Apr. 2009.
[26] D. W. Hoffman and J. A. Thornton, “Internal stresses in sputtered chromium,” *Thin Solid Films*, vol. 40, pp. 355 – 363, 1977.
[27] J. E. Yehoda and R. Messier, “Are thin film physical structures fractals?,” *Appl. Surf. Sci.*, vol. 22–23, Part 2, pp. 590 – 595, 1985.
[28] J. Laconte, D. Flandre, and J.-P. Raskin, “Thin dielectric films stress extraction,” *Micromachined Thin-Film Sens. SOI-CMOS Co-Integr.*, pp. 47–103, 2006.
[29] U. Helmersson, M. Lattemann, J. Bohlmark, A. P. Ehiasarian, and J. T. Gudmundsson, “Ionized physical vapor deposition (IPVD): A review of technology and applications,” *Thin Solid Films*, vol. 513, no. 1–2, pp. 1–24, Aug. 2006.
[30] H.-U. Krebs, M. Weisheit, J. Faupel, E. Süske, T. Scharf, C. Fuhse, M. Störmer, K. Sturm, M. Seibt, H. Kijewski, and others, “Pulsed Laser Deposition (PLD)–A Versatile Thin Film Technique,” in *Advances in Solid State Physics*, Springer, 2003, pp. 505–518.
[31] N. Savvides and B. Window, “Unbalanced magnetron ion-assisted deposition and property modification of thin films,” *J. Vac. Sci. Technol. A*, vol. 4, no. 3, pp. 504–508, 1986.
[32] A. Celler, X. Hou, F. Bénard, and T. Ruth, “Theoretical modeling of yields for proton-induced reactions on natural and enriched molybdenum targets,” *Phys. Med. Biol.*, vol. 56, no. 17, p. 5469, 2011.